Junior Nanotech Network 2012

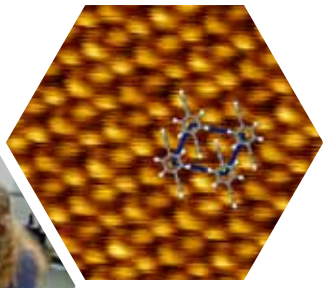

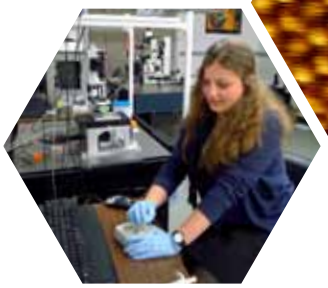

A Self-Organized
Graduate Student
Exchange Program

CNSI
CALIFORNIA NANOSYSTEMS INSTITUTE

CeNS
Center for NanoScience | LMU

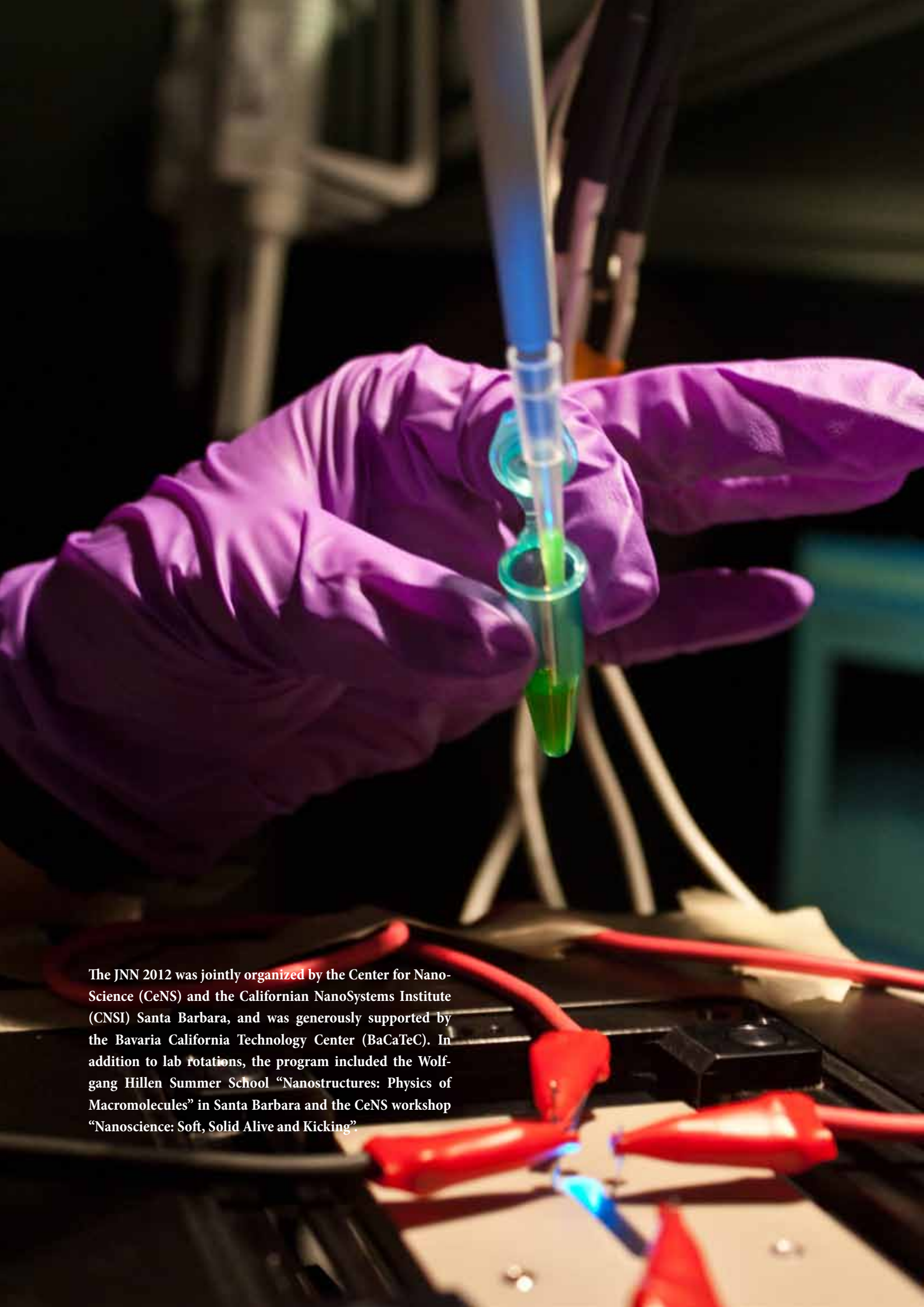

The JNN 2012 was jointly organized by the Center for Nano-Science (CeNS) and the Californian NanoSystems Institute (CNSI) Santa Barbara, and was generously supported by the Bavaria California Technology Center (BaCaTeC). In addition to lab rotations, the program included the Wolf-gang Hillen Summer School "Nanostructures: Physics of Macromolecules" in Santa Barbara and the CeNS workshop "Nanoscience: Soft, Solid Alive and Kicking".

Contents

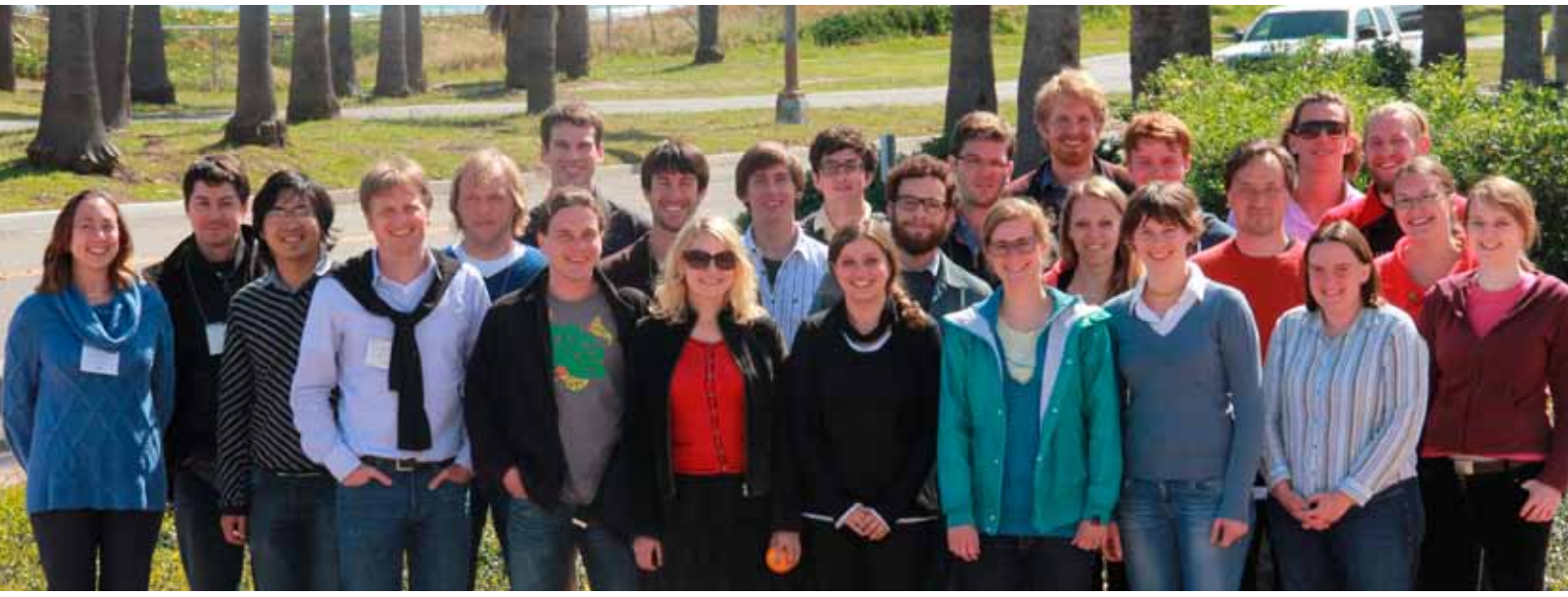

Participants of the JNN 2012:
Top Row (l-r): *Colin Fellows (UCSB), John Berezney (UCSB), Markus Stallhofer (CeNS), Dustin McIntosh (UCSB), Philipp Nickels (CeNS), Michael Isaacman (UCSB), Paul Zakrevsky (UCSB);*
Middle Row (l-r): *Prof. Tim Liedl (CeNS), Chris Carach (UCSB), Alex Heilman (UCSB), Jackson Travis Del Bonis-O'Donell (UCSB), Johanna Eichhorn (CeNS), Prof. Dieter Braun (CeNS, speaker at the JNN Symposium in Santa Barbara), Svenja Lippok (CeNS);*
Bottom Row (l-r): *Prof. Deborah Fygenson (UCSB), Prof. Vincent Noireaux (University of Minnesota, speaker at the JNN Symposium in Santa Barbara), Di Kang (UCSB), Prof. Alexander Holleitner (CeNS), Florian Strobl (CeNS), Ida Pavlichenko (CeNS), Mehrije Ferizi (CeNS), Sonja Schmid (CeNS), Kamila Klamecka (CeNS), Kimberly Weirich (UCSB), Susanne Seidel (CeNS).*

Welcome

Exchange of knowledge and collaboration between highly-skilled specialists promotes top-level research and new scientific developments. This generally accepted statement is especially true in Nanoscience, an area of research that is interdisciplinary by nature and often relies on merging the expertise of scientists from diverse fields, such as physics, chemistry, biology and material sciences. Ways of fostering scientific exchange differ widely. One successful method is to organize meetings in which established researchers present their latest achievements. However, students participate only passively in such meetings. It is therefore important to supplement meetings with an approach that engages the dynamics of young and enthusiastic students. Therefore the Center of NanoScience (CeNS) at LMU and the Californian NanoSystems Institute (CNSI) at UCSB worked together to realize the 4th Junior Nanotechnology Network (JNN), in which ten PhD students from each institution individually planned and realized experiments to introduce their research to one another, and spent two weeks each rotating through the laboratories of their foreign counterparts. This direct exchange of knowledge and expertise between PhD students is extremely efficient and, maybe more importantly, gives students a chance to explore new techniques, solidify their own skills by teaching them to others, and look at their own research and the research of others with fresh eyes.

The success of a JNN derives directly from the diligence, enthusiasm and open-mindedness of its student participants. This year's students spent many extra-hours in their laboratories, hosted their visiting counterparts in their homes and gave of their free time to organize guided trips on the weekends. For all this, and for their fearlessness in fully engaging in this endeavor, we thank all the participating students. We are also grateful to the group leaders and organizers at both CeNS and CNSI for supporting this JNN with their time and resources. By opening your labs and sharing your ideas, you implemented the spirit of open access and scientific exchange on all levels that fosters excellent research.

The hospitality and the scientific openness of all partners, both junior and senior, made this JNN exchange a true success and an invaluable experience. We are delighted with the surely long-lasting scientific and personal ties that were established, and we look forward to the development and realization of joint ventures and exciting ideas that they produce.

Prof. Tim Liedl
Center for NanoScience and LMU München, Germany

Prof. Deborah Fygenson
Californian NanoSystems Institute and University of Santa Barbara, U.S.A.

Prof. Alexander Holleitner
Center for NanoScience and Technische Universität München, Germany

About the Junior Nanotech Network

PhD students from the Center for NanoScience (CeNS, LMU Munich) teamed up with their peers from the University of California Santa Barbara (UCSB) for the 2012 round of the Junior Nanotech Network. The participants of the JNN were preselected based on excellence and compatibility of the proposed projects. In March/April, ten graduate students from Santa Barbara were the scientific and housing hosts for ten CeNS students for three weeks, while the German group hosted the UCSB students for a three week European visit in September.

Lectures and Lab work

The scientific programs in both locations comprised of two main elements: hands-on experimental training by the host peers and workshops including talks and posters by the PhD students. During the extended period of laboratory work, the students were acquainted with new techniques and were introduced to many different subjects in the nanosciences and biophysics. At the workshops, the participants heard presentations from internationally renowned speakers and were given the chance to present their own work and to engage in discussions with researchers from all over the world.

Learning from Peers

One interesting feature of the JNN is the self-organized character of the project. In particular, the PhD students were asked to design, teach, and supervise their scientific experiments independently. The laboratory work was carried out in small groups under the supervision of the host students. In this way, students coming from different areas of nanosciences were exposed to a variety of cutting-edge technologies. The scientific projects allowed the transfer of new technical skills and gave the hosts the opportunity to demonstrate their advanced research to an enthusiastic audience.

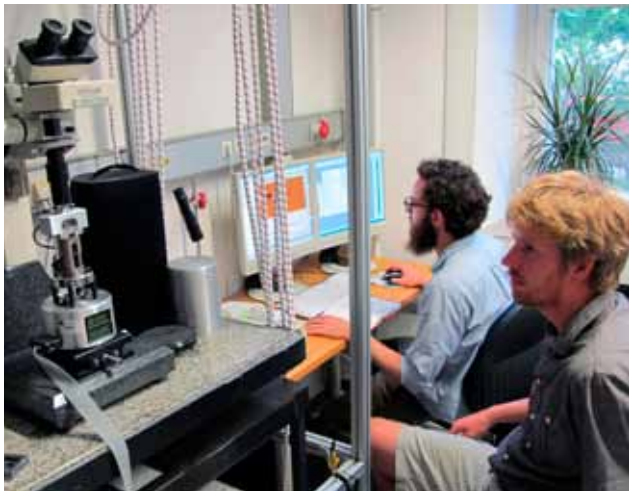

Intercultural Exchange

The scientific program was complemented and enriched by the social, cultural and outdoor activities which were organized by the host students. To guarantee the social integration of the guests, the visiting researchers were housed in the apartments of their local exchange partners. This close interaction fostered the intercultural exchange and stimulated informal scientific discussions. Combining joint lab work with common leisure activities enabled the creation of strong bonds between the students from the USA and Germany.

Workshops: Lectures and Scientific Discussions

Symposium in Santa Barbara

During the first part of the JNN exchange in Santa Barbara, a four-day symposium took place on the campus of the University of California Santa Barbara. This gave the German and the American participants the opportunity to present their own research, to familiarize with each other's research projects, to get feedback on the obtained results, which was an integral part of the exchange program. In addition, Prof. Melosch (Stanford University) and Prof. Noireaux (University of Minnesota) as well as UCSB faculty and CeNS faculty gave insight into their research in the field of nanoscience, covering topics such as artificial cells, microscopy with nanoscale resolution and nanostructures built from DNA.

The symposium also included a visit to the Nanotech nanofabrication 12,700 ft² clean room facility with lithography, thin-film deposition and reactive ion etching tools as well as CNSI research facilities for material properties' characterization.
Apart from the vivid scientific interaction during the symposium, the students and the professors could enjoy informal discussions during the coffee and lunch breaks, discussing topics such as career planning or women in science in a relaxed and friendly atmosphere.

Workshop in Venice

During the second part of the JNN, the UCSB and CeNS PhD students were invited to participate in the CeNS Workshop "Nanosciences: Soft, Solid, Alive and Kicking" at Venice International University, Italy. CeNS welcomed 27 internationally renowned speakers to the sunny and beautiful island of San Servolo for five days of intense exchange on the topic of the nanosciences. In their stimulating talks, speakers from all over the world presented an overview of current research topics on nanometer-scale science and presented their latest research highlights. As usual at the annual CeNS workshops, a wide assortment of research areas was covered: from biophysics, quantum optics and hybrid technologies to nanomaterials

among many others. These talks provided an excellent overview and complemented the narrow perspective of one's own research field.
The JNN participants had the opportunity to join in many lively discussions with internationally renowned researchers as well as with their fellow CeNS students from the fields of physics, chemistry and biology taking place inside of the lecture hall, but also during the poster sessions and breaks on the green yards of San Servolo.

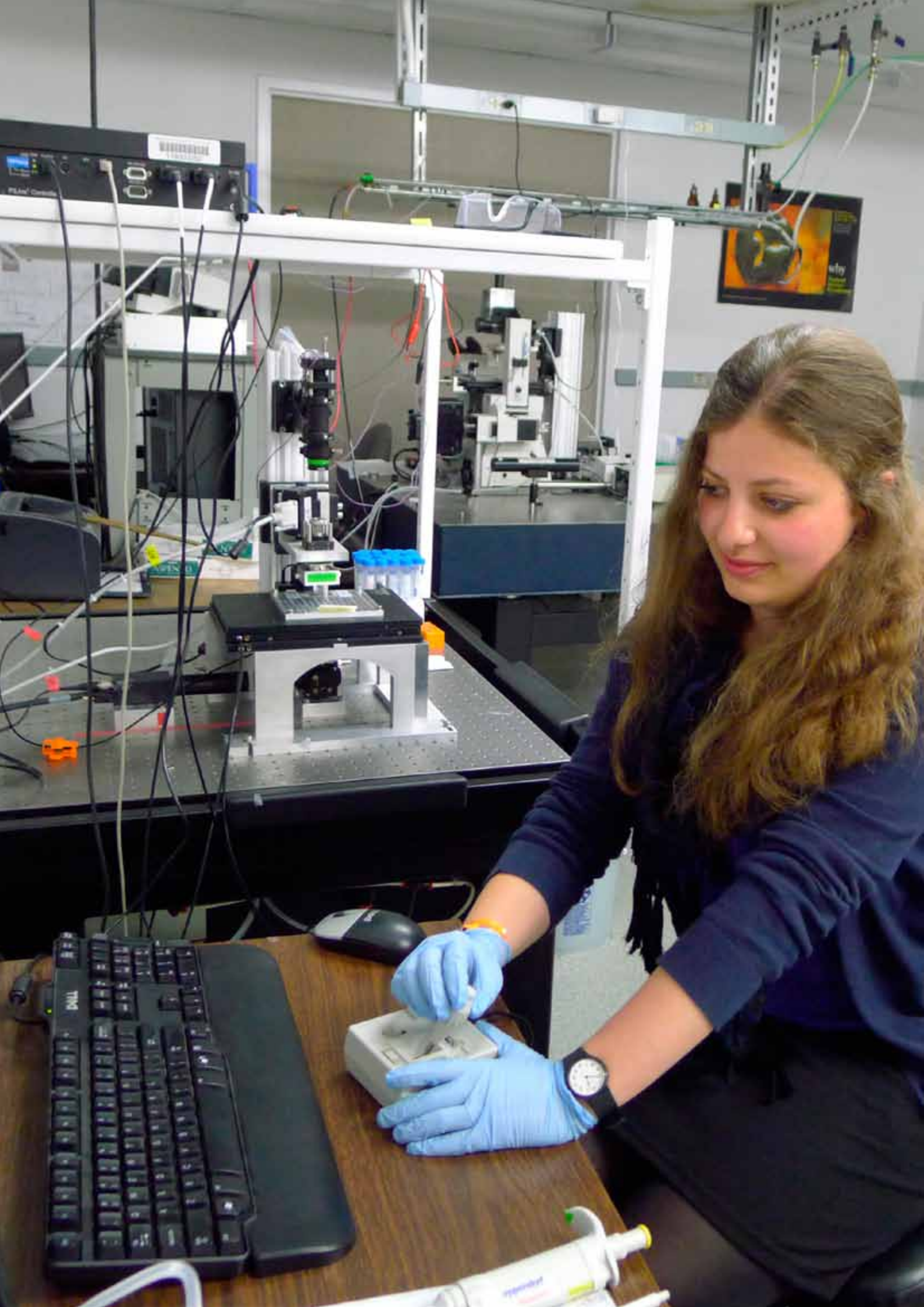

Research Projects

SVENJA LIPPOK

Fluorescent Correlation Spectroscopy Measurements of von Willebrand Factor

Fluorescence Correlation Spectroscopy (FCS) is based on a confocal fluorescence setup and can be used to analyze the dynamics of macromolecules by detecting the intensity time trace of fluorescent molecules diffusing in and out of the small optical confocal volume. It allows for measuring hydrodynamic radii and particle concentrations in buffer as well as in more complex media like blood plasma. Therefore it is possible to monitor molecules in their native environment that strongly influences their biological function. This project started with an introduction to our setup measuring correlation curves of different well-known biomolecules. We discussed analysis procedures and the underlying theory. We proceeded with measurements dealing with my up-to-date research project which is the size distribution analysis of Von Willebrand Factor (VWF), a polymer essential for blood coagulation.

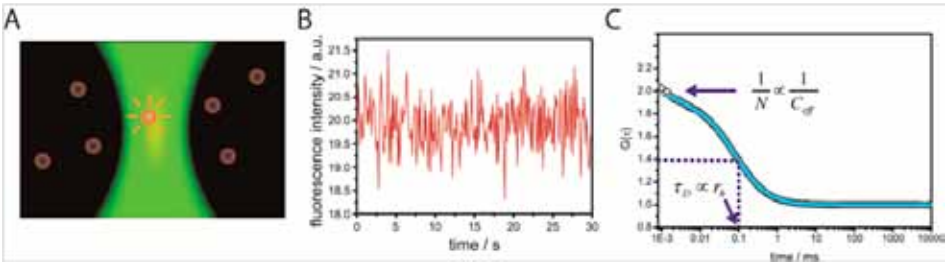

Fig. 1: *Schematic representation of FCS: Fluorescence emitted by molecules in a confocal observation volume (A) is detected as fluctuating intensity signal due to Brownian motion of the molecules (B). Correlation analysis of this intensity trace provides information about hydrodynamic radii and particle concentrations (C).*

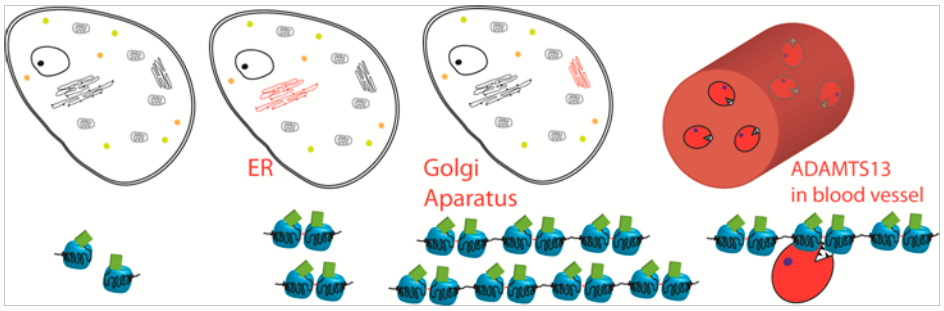

Fig 2: *Polymerization of VWF is completed in different compartments of the cell. After secretion to the blood, VWF size is regulated by the protease ADAMTS13.*

VWF is a multifunctional polymer that exists with a variable number of dimeric subunits. Its functionality is highly dependent of its size why shifts to smaller polymer sizes indicate pathological VWF function. Hence research about the underlying polymerization mechanism is of huge importance to understand how malfunctioning size distributions are created which provides the basis for new treatments of bleeding disorders.

Contact

Svenja Lippok
Rädler group
Physics Department
LMU München
Geschwister-Scholl-Platz 1
80539 Munich
svenja.lippok@physik.uni-muenchen.de

SONJA SCHMID

Conformational Protein Dynamics by Single-Molecule FRET

Proteins are commonly called the molecular machines of our body. While some proteins actually turn chemical energy into mechanical forces, others act as chemical catalysts, signal transducers or structural building blocks. Nevertheless, all proteins share the fact that their function is determined by their 3d structure. We are interested in conformational motion within these large molecules and ways to influence it. We study these single molecule effects by TIRF using FRET as a molecular ruler.

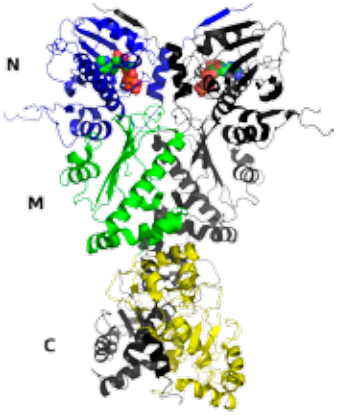

Fig. 1: *Crystal structure of Hsp90 (pdb: 2CG9).*

Heat-shock protein 90 (Hsp90) is a protein that shows large thermally-driven conformational changes - even in the absence of any other energy source. In yeast, this chaperone protein helps client proteins to fold into their native structure in an ATP dependent way.

As shown in Fig. 1, it consists of two identical protomers each composed of an N-terminal, a middle and a C-terminal domain. Opposing N- and M-domains fluctuate between the depicted closed and a more open conformation.

We are interested in the energetics, the structural basis, as well as, the function of such movements. Since these fluctuations are not synchronized within the ensemble, single-molecule techniques must be applied to get quantitative information. To this end, we exploit Förster Resonance Energy Transfer (FRET) between two fluorescent probes that are attached to the protein at specific positions. The fluorescence signal is then measured by a single-molecule Total Internal Reflection Fluorescence microscope (smTIRF) (s. Fig. 2). This allows for excitation of single Hsp90 molecules through the evanescent field at the glass-water interface.

From the recorded fluorescence signals, we can extract information about the distance between the two fluorophores over time. Fig. 3 shows characteristic time traces of single Hsp90 molecules. The calculated FRET efficiency is indicative of the protein conformation. The FRET histogram (Fig. 4) shows that two states are predominantly populated, representing an open and a closed conformation.

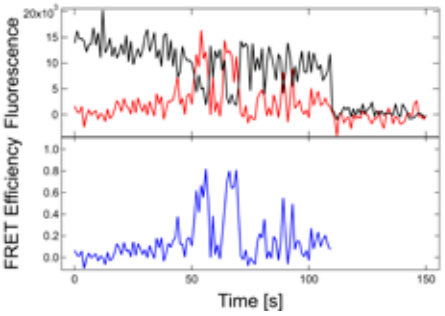

Fig. 3: *Time traces of fluorescence and energy transfer efficiency between two protomers of a single Hsp90. High or low FRET is indicative of a closed or open conformation, respectively.*

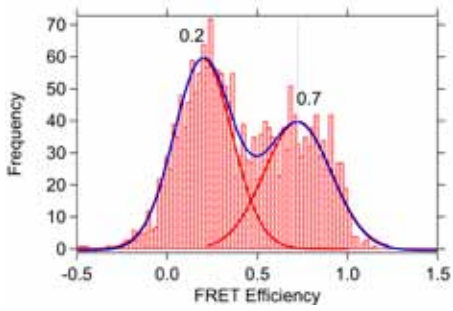

Fig. 4: *The histogram of 23 FRET traces reveals two predominantly populated states: open and closed.*

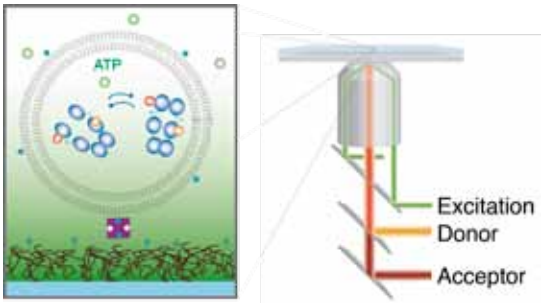

Fig. 2: *Illustration of vesicle immobilized Hsp90 and the optical path in an objective-type TIRF setup.*

Contact

Sonja Schmid
Hugel group
Dept. Physics E22a
Technical University Munich
James-Franck-Str. 1
85748 Garching
sonja.schmid@tum.de

DUSTIN MCINTOSH

Elastic Response of DNA Molecules

Single-molecule force spectroscopy via magnetic tweezers is a strategy for examining the mechanical properties of polymer molecules in solution. Here, we examine what this technique can tell us about the structure of DNA in both its double-and single-stranded forms (dsDNA and ssDNA). Rigid dsDNA is well-described as an ideal, semi-flexible polymer, while flexible ssDNA markedly deviates from all ideal predictions at low force.

In this experiment, students are introduced to single-molecule force spectroscopy with magnetic tweezers (see Fig. 1). In this technique, single polymer molecules are tethered between a glass surface and a micron-sized paramagnetic bead. Using macroscopic external permanent magnets, we apply a magnetic field gradient to the bead, exerting a force and stretching the polymer. The resulting force-extension data can be easily compared to theoretical models providing insight into the polymer's mechanical properties.

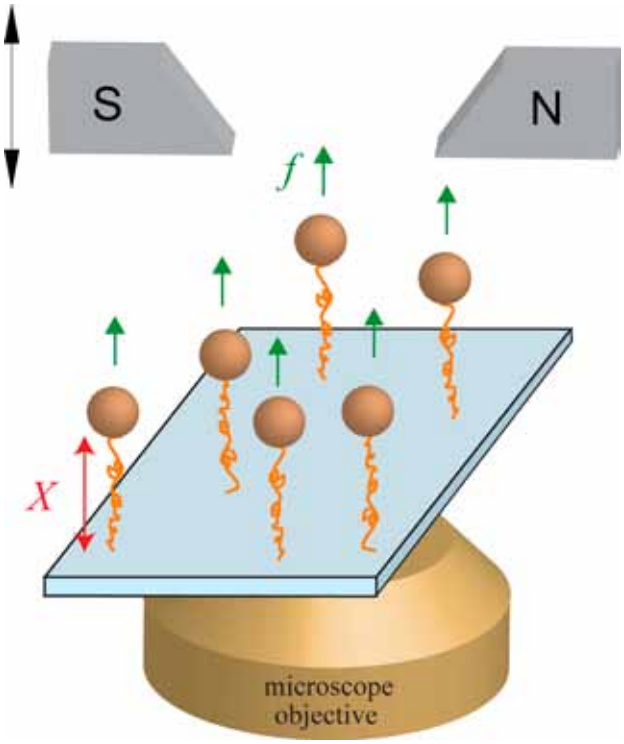

Fig. 1: *Sketch of magnetic tweezers.*

The experimental procedure begins with flow cell construction and DNA synthesis. The flow cell consists of two glass cover slips sandwiching a piece of parafilm patterned with a laser cutter. One of the cover slips is smaller than the other allowing the user to manually pipette and wick solution through the flow cell (see Fig. 2A). The dsDNA substrate (lambda DNA) is annealed at either end to functionalized ssDNA oligomers for immobilization (see Fig. 2B). ssDNA is created by Rolling Circle Amplification: a primer oligomer is annealed to a circularized template oligomer. A polymerase enzyme can then extend the primer, rolling along the template repeatedly, forming a long ssDNA of repeating sequence (see Fig. 2C). With appropriate design of the template sequence, secondary structure can be avoided to test the entropic elasticity of ssDNA.

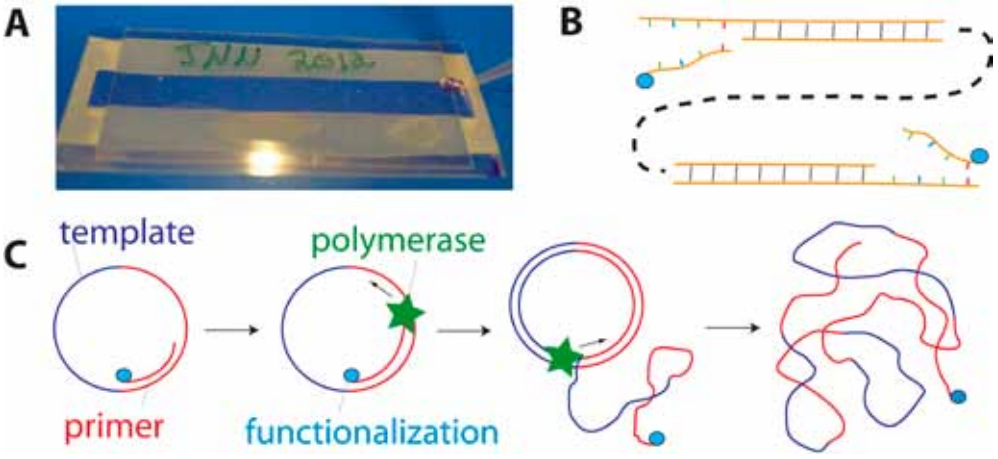

Fig. 2: *A. A simple flow cell for single-molecule manipulation. B. Synthesis of functionalized dsDNA by oligo annealing. C. Synthesis of functionalized ssDNA by Rolling Circle Amplification.*

Stretching these polymers in the magnetic tweezers results in the force-extension data plotted in Fig. 3. These data reveal that dsDNA is significantly more rigid than ssDNA. Comparison with the Marko-Siggia Worm-Like Chain model [1] reveals that dsDNA has a 50 nm persistence length. ssDNA, on the other hand, does not adequately fit to the Worm-Like Chain. In fact, at the lowest forces, where the polymer is significantly coiled upon itself, ssDNA's elastic response is nonlinear, in contrast to ideal elasticity, indicating the influence of long-range excluded volume interactions in a "real" polymer [2].

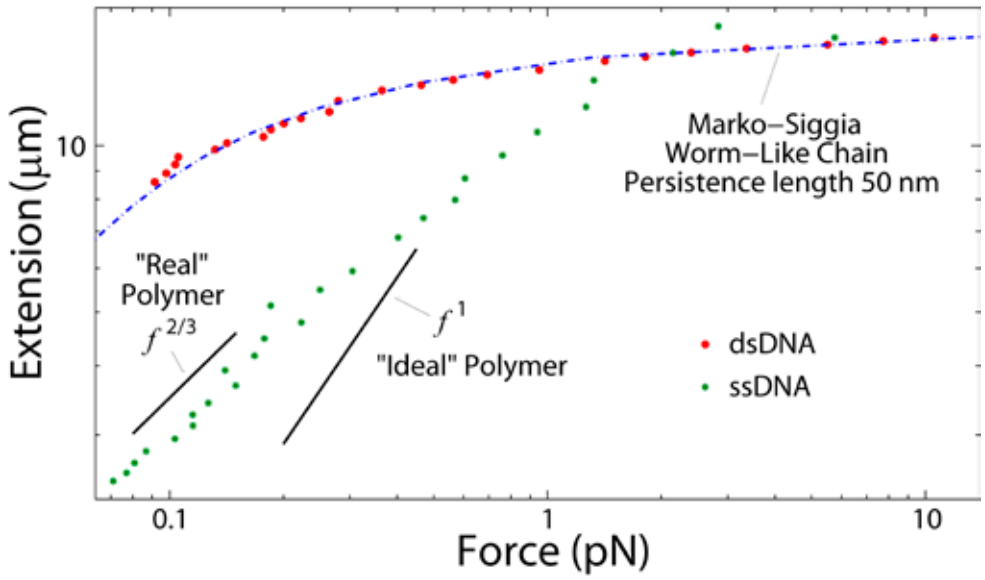

Fig. 3: *Force-Extension data for dsDNA and ssDNA compared with theoretical models. dsDNA is a semi-flexible ideal polymer, but ssDNA deviates significantly from ideal predictions but is consistent with predictions for "real" polymer elasticity.*

References:

1. J. F. Marko and E. D. Siggia, Macromolecules 28, 8759 (1995).
2. P. Pincus, Macromolecules 9, 386 (1976).

Contact
Dustin McIntosh
Saleh group
Department of Physics
University of California Santa Barbara
Eng. Materials Dept. Bldg. 503 Rm. 1355
Santa Barbara, CA 93106-5050
dmcintos@physics.ucsb.edu

JACKSON TRAVIS DEL BONIS-O'DONNELL

Electrokinetic Behavior of Fluorescent Ag:DNA Nanoclusters in Microfluidic Flows

Electrokinetic –based microfluidic devices have been demonstrated as powerful bioanalytical tools for the separation and identification of various fluorescently tagged biomolecular compounds. For this module, we use microfluidic separations in cross-channel geometry fused silica microchannels to study novel silver-DNA based fluorophores. Silver-DNA nanoclusters (Ag:DNA) are hybrid macromolecules in which a silver superatom is stabilized by segments of single stranded DNA in aqueous solution. The clusters fluoresce at wavelengths that can be tuned across the visible spectrum by varying the DNA sequence. The combination of their small size and tunable spectra opens exciting, new possibilities for biological imaging, medical diagnostics and the development of self-assembled DNA nanotechnologies. While spectral information is easily obtained from Ag:DNA synthesized in bulk, detailed information about their internal structure requires arduous purification and has been limited by the resulting low yield.

Recently, electrokinetic separations in microchannels have proven useful for measuring the size and charge of different fluorescent Ag:DNA emitters stabilized by the same sequence of DNA. Small (~50-100 pL) sample plugs are electrokinetically injected down a 30 mm long, 20 μm deep silica channel in the presence of a buffered background-electrolyt. Fluorophores contained within the injected plug travel at different velocities and thus separate down the length of the separation channel due to their differences in electrophoretic mobility. Diffusion measurements are also performed in situ by watching the time evolution of a stationary fluorescent sample plug.

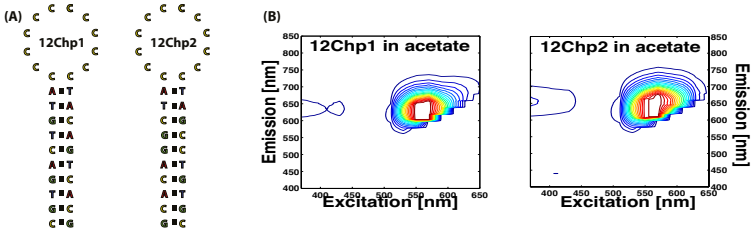

Fig. 1: *(A) Schematic depicting the sequences of 12-cytosine DNA hairpins used in this study. (B) Excitation- emission matrices depicting the fluorescent spectra of 12C hairpin Ag:DNAs obtained from a bulk sample using a Tecan Infinite200 platereader. The fluorescence spectra reveal that both samples emit strongly in red.*

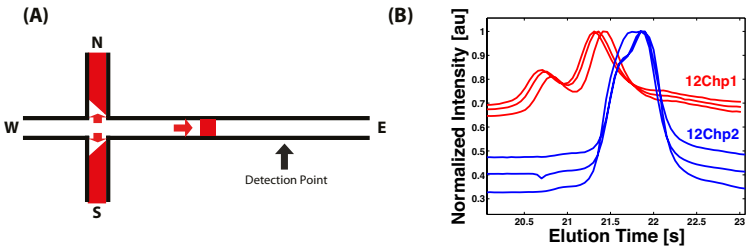

Fig. 2: *(A) Schematic diagram depicting sample plug eluting down separation channel in a microfluidic device. Sample is driven from north to south using an applied electric field provided by a high voltage sequencer. The voltages are then switched to drive a sample plug east down the separation and detection channel. (B) Normalized fluorescence intensity recorded by a CCD as a function of elution time of 12Chp1 and 12Chp2 down a 20 μm deep silica channel. Discernible peaks indicate multiple Ag:DNA species are contained within a single sample. Multiple trials demonstrate repeatability of measurements.*

For this module, the above techniques are applied to Ag:DNA stabilized by different sequences of DNA designed to adopt the same structure: a 12 cytosine single-stranded loop. Module attendees first synthesize red-emitting Ag:DNA fluorescent nanoclusters using several different sequences of DNA and measure fluorescence emission using a Tecan Infinite 200Pro plate reader. Samples of each fluorophore are then analyzed by performing electrokinetic separations in a microfluidic device using an Olympus IX70 inverted fluorescence microscope, mercury excitation source and Andor iXon+ EMCCD camera. The resulting video microscopy data is analyzed using custom Matlab analysis software to calculate the velocity and mobilities of fluorescent species in the sample.

Contact

Jackson Travis Del Bonis-O'Donnell
Pennathur group
Department of Mechanical Engineering
University of California Santa Barbara
Santa Barbara, CA 93106-5050
jtdo@engineering.ucsb.edu

PHILIPP NICKELS

DNA Origami Structures Folded Directly from Virus Particles

DNA origami is a widely used method for the self-assembly of nanoscale objects with addressable features of unprecedented levels of positional accuracy. This technique employs a virus-based DNA single strand as a scaffold which is brought into shape by hundreds of short oligonucleotides. The achievable size of structures built with the original origami method is limited by the size of the single-stranded scaffold molecule used. Scaling up the size of DNA origami structures remains a critical challenge that is facing the further development of DNA origami technology. Building large objects approaching the size scale of conventional photolithography techniques might be a feasible approach to combine bottom-up self-assembly with top-down lithography. Currently, the methods for the production of single-stranded DNA molecules are less efficient than those for double-stranded DNA. For the assembly of DNA Origami structures the single-stranded genome of the bacteriophage M13 usually serves as a scaffold molecule. Here we present the use of the double-stranded genome of the bacteriophage λ as a source of scaffold. We show that it is possible to assemble the structures directly from the bacteriophage particles without further purification methods of the scaffold material. To prove the versatility of the method we show that it is also possible to assemble conventional DNA origami structures from bacteriophage M13 particles. The origami structures are assembled and characterized via agarose gel electrophoresis and atomic force microscopy (AFM).

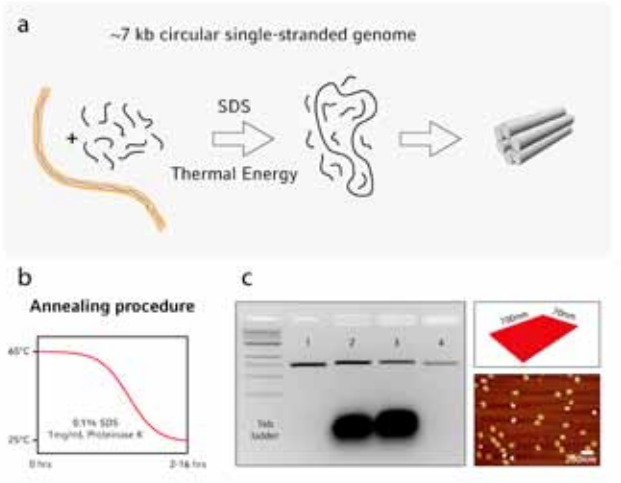

Fig. 1: (a) Schematic overview of folding from bacteriophage M13 particles: the phage particles are mixed with staples, buffer, and SDS. The sample is exposed to a thermal annealing ramp. (b) The structures are assembled via a nonlinear annealing ramp that starts at 65°C and goes down to room temperature. Proteinase K is added to digest the denatured phage proteins. (c) Characterization of the assembled origami structures via gel electrophoresis and AFM.

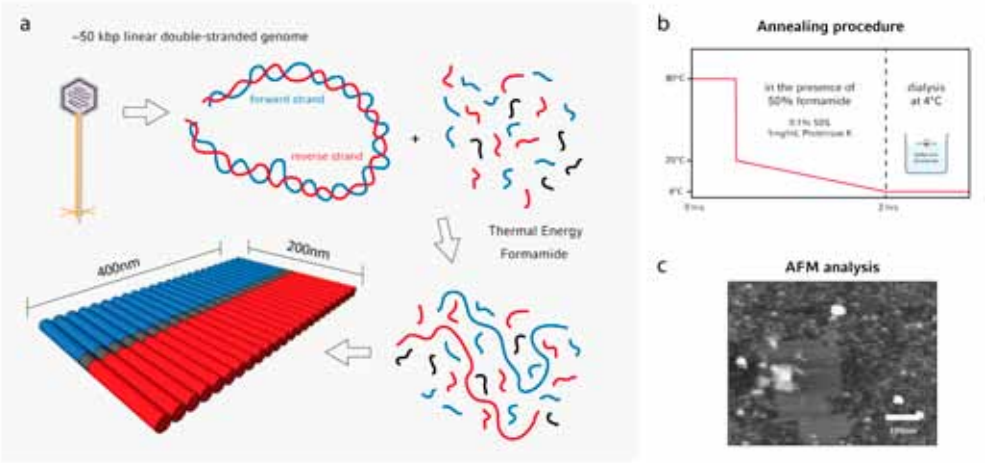

Fig. 2: (a) Schematic overview of folding from bacteriophage λ particles: the phage particles are mixed with 3 different sets of staples, buffer, formamide, and SDS. The sample is exposed to a thermal annealing ramp to assemble the structures: the blue/red staples fold the forward/reverse strand into parts of the structure, respectively. The black staples connect the two parts. (b) The mixture is heated to 80°C. In the presence of formamide the double-stranded DNA is denatured. A quick temperature jump prevents re-annealing of the scaffold. The dialysis step removes the formamide from the sample (c) AFM image of the assembled structure.

Contact

Philipp Nickels
Liedl group
Physics Department
Ludwig-Maximilians-Universität München
Geschwister-Scholl-Platz 1
80539 Munich
philipp.nickels@physik.lmu.de

MARKUS STALLHOFER

Optoelectronic Characterization of Nanoscale Circuits

In order to analyze the optoelectronic properties of nanoscale circuits, we focus a laser through a confocal microscope onto such circuits. Then, we scan the laser spot across the circuit and simultaneously measure the optical beam induced current (OBIC) through a quantum point contact (QPC). QPCs are one-dimensional constrictions in electronic circuits, and they exhibit a conductance quantized in steps of $2e^2/h$. With this technique, quasi-ballistic photocurrents in the nanoelectronic circuits can be visualized and characterized. In addition, quantized photocurrents across the QPC can be probed and manipulated.

Utilizing the OBIC technique, we spatially resolve and analyze the non-equilibrium flow-patterns of photogenerated electrons in a GaAs based two-dimensional electron gas (2DEG) at a perpendicular magnetic field, as shown in Fig. 1 [1, 2]. We observe laterally curved trajectories with a radius being inversely proportional to $|B|$, as expected for cyclotron motion. However, the radii of the measured trajectories are 10 to 30 times larger than anticipated. Both the experimental findings and Monte Carlo simulations suggest that due to an enhanced influence of electron-electron scattering, the radius of the trajectories of hot electrons is generally enlarged.

Furthermore, the extracted propagation length of the photogenerated electrons in the 2DEG depends non-monotonically on the laser intensity [3]. For the lowest excitation intensities, we determine a quasi-ballistic transport regime in which the measured propagation length of the photogenerated electrons approaches the mean free path l_{mfp} of the 2DEG without laser excitation. With increasing excitation intensity, this propagation length decreases because of an increased scattering phase space and, finally, it increases again due to screening of momentum scatterers at higher densities of the photogenerated electrons. Our observations underline the predominant influence of scattering and screening processes in mesoscopic and nanoscale photodetectors.

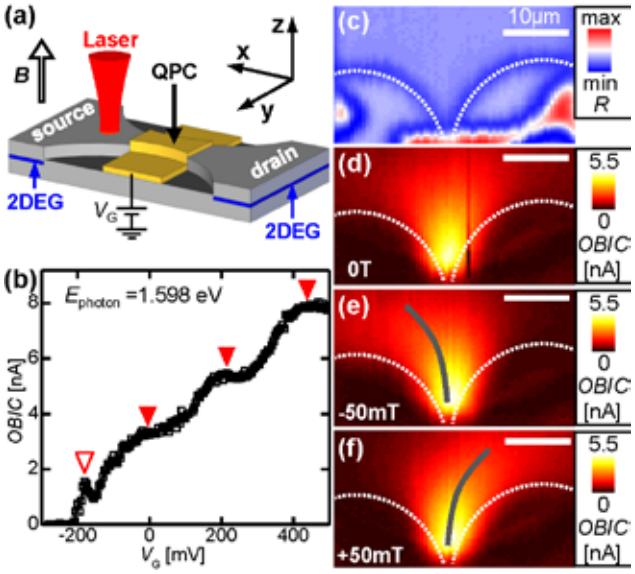

Fig. 1: *(a) Experimental method. (b) Optical Beam Induced Current (OBIC) as function of V_G. Quantization steps reveal one-dimensional subbands (filled triangles). (c) Spatially resolved reflection map. (d)-(f) Spatial map of OBIC for (d) $|B|$= 0 T, (e) -50 mT, and (f) 50 mT (Images taken from reference [2]).*

In the JNN lab course, we discussed the theoretical background and the sample fabrication, took a detailed tour through our cleanroom facilities, and performed low-temperature photocurrent experiments on a QPC sample.

References:

1. K.-D. Hof, F. J. Kaiser, M. Stallhofer, D. Schuh, W. Wegscheider, P. Hänggi, S. Kohler, J. P. Kotthaus, A. W. Holleitner, Nano Letters 10, 3836 (2010).

2. M. Stallhofer, C. Kastl, M. Brändlein, D. Schuh, W. Wegscheider, J. P. Kotthaus, G. Abstreiter, A. W. Holleitner, Phys. Rev. B 86, 115315 (2012).

3. M. Stallhofer, C. Kastl, M. Brändlein, C. Karnetzky, D. Schuh, W. Wegscheider, A. W. Holleitner, Phys. Rev. B 86, 115313 (2012).

Contact
Markus Stallhofer
Holleitner group
Walter Schottky Institut
Technische Universität München
Am Coulombwall 4
85748 Garching
Markus.Stallhofer@wsi.tum.de

JOHANNA EICHHORN

Surface-Confined Self-Assembly of Organic Molecules

Molecular self-assembly on surfaces is a promising approach for the efficient synthesis of functional two-dimensional nanostructures. Monolayer deposition of organic molecules on different substrates is a bottom-up technique capable of producing two-dimensional networks with tunable and well defined properties. Moreover, surfaces can be structured and functionalized in order to control and enhance their electronic or optoelectronic properties for nanotechnological applications.

In my JNN project, we used Scanning Tunnelling Microscopy (STM) to study self-assembled monolayers of 1,4-diethynylbenzene (DEB, Figure 1), a double ethynyl functionalized benzene ring, on a metal substrate. All experiments were carried out under ultra-high vacuum conditions, whereby these well defined and clean conditions minimize surface contamination.

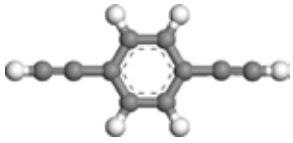

Fig. 1: *Molecular structure of 1,4-diethynylbenzene.*

In the first part, we deposited the molecules on a previously cleaned Cu(111) surface by means of a precision leak valve. A metal capillary was connected to the valve to guide the molecules to the substrate (Figure 2). Equipped with appropriate functional groups (H-C≡C-), the adsorbed molecules spontaneously self-assemble into ordered monolayers on the surface. The driving force for DEB self-assembly are electrostatic dipole-dipole interactions ($-C\equiv C-H\cdots-C\equiv C-$) arising from the polarization of the ethynyl group (Figure 3).

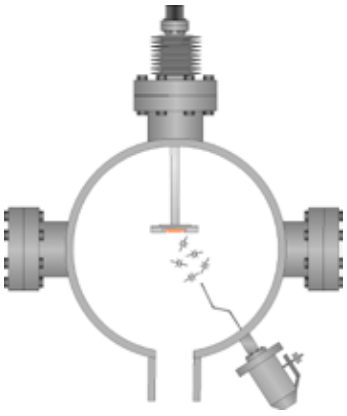

Fig. 2: *Preparation scheme.*

Fig. 3: *$-C\equiv C-H\cdots-C\equiv C-$ interactions and polarization of the ethynyl group*

In the second part, we investigated the DEB monolayer by means of a Scanning Tunneling Microscope. For all experiments, STM tips were electrochemically etched from a tungsten wire. This technique allows imaging of structures with high resolution down to the nanometer scale. Single molecules and even submolecular features can thus be resolved, whereby morphology and symmetry of monolayers as well as their lattice parameter and intermolecular distances can be determined. An STM image of the self-assembled DEB monolayer on Cu (111) is depicted in Figure 4. The overlaid tentative model shows the orientation of the molecules and the blue lines one unit cell.

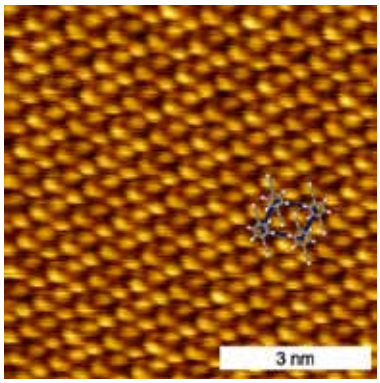

Fig. 4: *STM topography of a self-assembled 1,4-diethynylbenzene monolayer on Cu(111).*

Contact

Johanna Eichhorn
Lackinger Group
Technische Universität München
Deutsches Museum
Museumsinsel 1
80538 München
johanna.eichhorn@tum.de

ALEX HEILMAN

Graphene 101: An Introduction to Synthesis, Transfer and Characterization

Graphene, a single layer of sp^2 hybridized carbon, has garnered considerable attention in the scientific community since its initial discovery in 2004 because of its unique mechanical, electrical and optical properties. Characteristics such as ultra-high tensile strength, strong fluorescence quenching, atomic thickness and optical transparency not only make graphene an interesting material system to study but also suggest that it could make an excellent substrate for the near-field optical experiments done in our lab. The goal of this module was to give the participants an introduction to some of the basic principles and procedures used in the synthesis and characterization of graphene by having them grow and transfer graphene films and use atomic force microscopy and Raman spectroscopy to assess their quality.

Synthesis

Graphene samples were synthesized via chemical vapor deposition (CVD) of methane on catalytic copper foils in a home-built furnace (Figure 1) that allows control of key parameters, such as temperature, pressure and gas concentrations. Copper samples were first annealed at 1035°C under a reducing atmosphere, then methane was introduced, initially in low concentrations, to nucleate graphene crystals on the copper surface. The concentration was incrementally increased to grow these crystals until the entire surface was covered with roughly a monolayer of graphene.

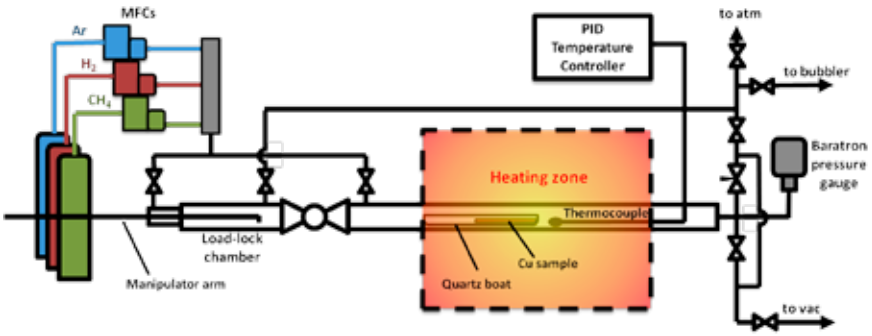

Fig. 1: *Schematic of furnace used for CVD growth of graphene on Cu substrates.*

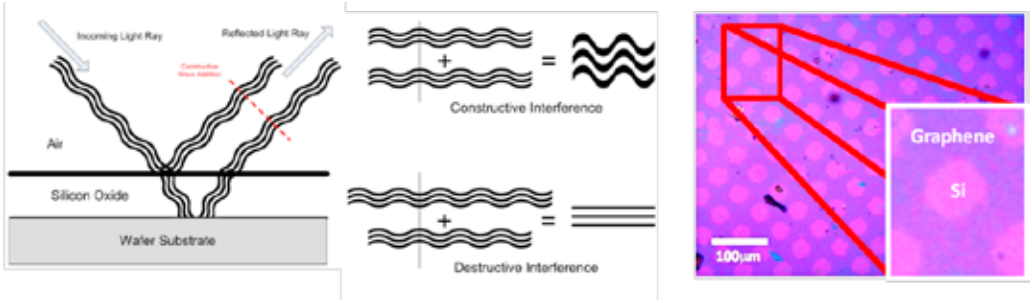

Fig. 2: *Interference between light reflected at the air/surface and the SiO_2/Si interfaces gives rise to color contrast between areas with and without graphene on the surface.*

Transfer

Due to the rough surface texture and considerable optical background of the Cu substrates, it was necessary to transfer the graphene samples to silicon wafers for characterization by AFM and Raman spectroscopy. An additional benefit of this transfer is that it allows direct visualization of the atomically thin monolayer via optical interference (Figure 2). By transferring the graphene to Si wafers with a 300nm surface oxide layer, the added thickness from the graphene changes the wavelength required for constructive interference (as per Bragg's Law: $n\lambda=2d\sin\theta$), giving the graphene a purple appearance on the pink background. As part of the module, this 300nm oxide layer was grown via thermal oxi-

dation in a tube furnace at 1050°C in the presence of N_2, O_2 and steam for 3 hours. Graphene films were transferred from the Cu growth substrates to the oxidized Si using the method shown in Figure 3. A thin protective layer of PMMA was spun on the Cu/graphene surface, and an O_2 plasma was used to etch the undesired graphene from the opposite side of the sample. A 0.1M ammonium persulfate solution was then used to etch the Cu from underneath the graphene, leaving a thin graphene/PMMA layer floating on the surface of the solution. After extensive rinsing, the graphene/polymer film was collected on the oxidized Si and the polymer was removed by soaking overnight in acetone, leaving behind the atomically thin monolayer of graphene on the Si wafer.

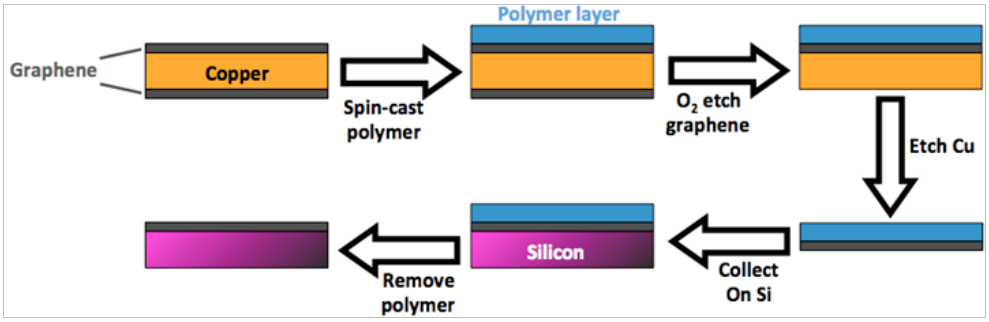

Fig. 3: Schematic of the procedure used to transfer graphene layers from Cu onto Si.

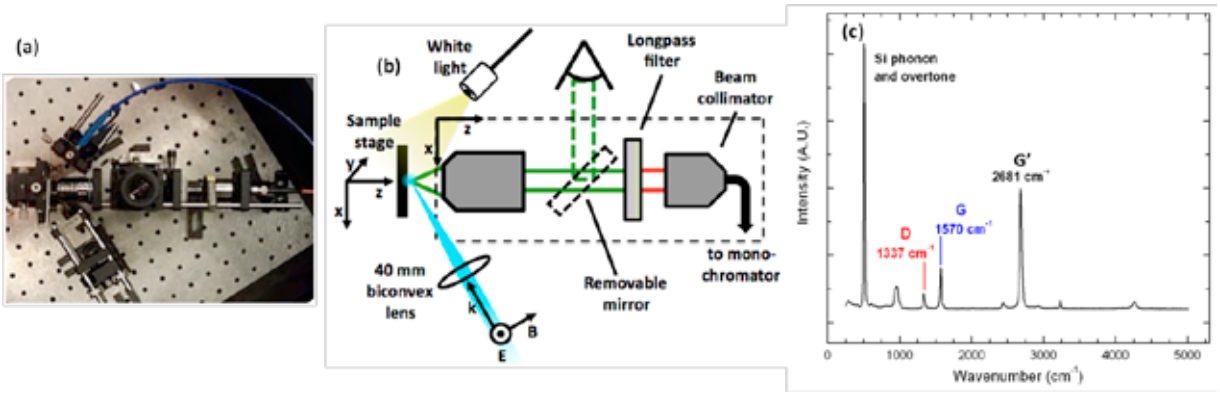

Fig. 4: (a) Image and (b) schematic of the microscope used to collect Raman spectra of graphene. (c) Raman spectrum of graphene on Si showing the graphene's three fundamental Raman peaks: D at ~1350cm^{-1}, G at ~1580cm^{-1} and G' at ~2700cm^{-1}.

Characterization

Two techniques were used to characterize the graphene samples after transfer: Raman spectroscopy and atomic force microscopy (AFM). Raman spectroscopy is a technique that uses inelastic scattering (Raman scattering) to detect the excitation of bond vibrations in materials, providing information comparable to IR absorption spectroscopy. Raman spectroscopy is commonly used to evaluate the quality of graphene samples because several important morphological properties, such as the number of layers and defect concentration, are born out in graphene's Raman signature. Using a simple microscope setup and 488nm laser light, far-field Raman spectroscopy was performed on the graphene samples (Figure 4). By assessing the intensity of the D peak at ~1350cm^{-1} (associated with defects in the graphene) and by comparing the intensities of the G' peak at ~2700cm^{-1} and the G peak at ~1580cm^{-1} (G':G ratio ~4:1 for monolayer graphene and ~1:1 for bilayer graphene), the quality of the graphene samples was determined.

Finally, atomic force microscopy was used to image the graphene samples. Analysis of step edge height profiles between graphene and bare Si allowed us to quantify the thickness of the graphene layers and, by comparison of these results with expected thicknesses, we could estimate the amount of residual polymer and other contamination on the samples.

Contact
Alex Heilman
Gordon group
Dept. of Chemical Engineering
University of California
Santa Barbara
Santa Barbara, CA 93106-5080
heilman@umail.ucsb.edu

SUSANNE SEIDEL

Biomolecular Interaction Analysis via Microscale Thermophoresis

Cell surface receptors recognize ligands. Transcription factors bind specific DNA motifs. Antibodies capture antigens. Pharmaceuticals work by binding their designated drug targets. These examples demonstrate, that specific interactions of biomolecules play a crucial role in all fields of life sciences. Our lab developed an innovative technique to quantitatively analyze these biological binding events: Microscale Thermophoresis (MST).

As the name already implies, the method is based on thermophoresis, the directed motion of molecules in a temperature gradient. Thermophoresis is highly sensitive to changes in size, charge and solvation shell. Since at least one of these parameters is affected by any biomolecular binding event, MST is successfully used for biomolecular interaction analysis (BIA). MST has several advantages compared to other well established BIA methods. As measurements are performed in free solution, time consuming immobilization procedures and the danger of surface artifacts, as e.g. present in surface plasmon resonance (SPR), are avoided. Compared to the "gold standard" of BIA, isothermal titration calorimetry (ITC), MST is characterized by a much lower sample consumption – a major advantage when working with precious biological material. It allows non-radioactive measurements in all kinds of liquids including biological fluids like blood serum. Such close to in vivo conditions significantly enhance the results' biological relevance. MST only requires one fluorescent binding partner. Besides attaching a fluorescent label, label-free measurements are also possible.

In the module both a fluorescence microscope which was modified in our lab for thermophoresis measurements and a commercially available MST instrument from our spin-off company Nanotemper were used. For measurements in either of these setups, the samples are transferred into glass capillaries and monitored via fluorescence excitation and emission (Fig. 1). A 1480 nm infrared heating laser is coupled into the light path. The water molecules within the sample absorb the infrared radiation. The generated temperature gradient induces thermophoretic motion: the biomolecules move away from or towards the heated spot.

A binding event that many scientists come across from time to time served as a first example: the binding of a primer to a DNA-template as known from PCR. For detection, the primer was labeled fluorescently. To infer binding affinity, a titration series was prepared, in which the concentration of the unlabeled template was varied, while the concentration of the fluorescently labeled primer was kept constant.

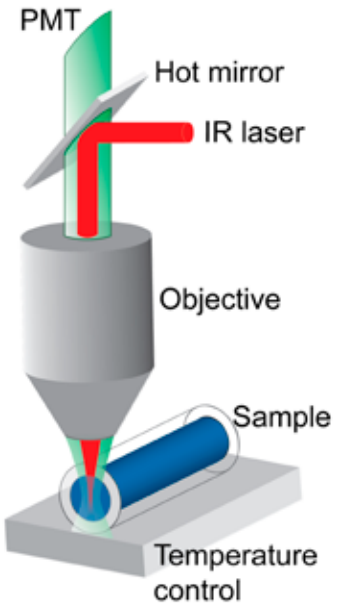

Fig. 1: *Thermophoresis setup. The sample is filled into a capillary and placed on a thermoelectric cooler providing a constant basis temperature. Fluorescence is excited with an LED and recorded with a photomultiplier tube (PMT). The solution inside the capillary is locally heated with an IR laser, which is coupled into the fluorescence microscope using an IR-reflecting "hot" mirror.*

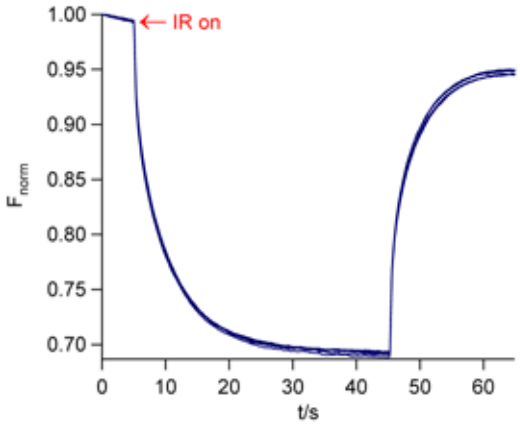

Fig. 2: *Fluorescence time traces. The initial fluorescence drops as soon as the IR-laser is turned on (t=5 s). This temperature jump on a 100 ms timescale depicts the fluorophore's temperature sensitivity. It can easily be separated from the following diffusion limited thermophoresis lasting several seconds. The unbound Cy5-labeled primer shows a weaker thermophoretic depletion than its complex with the DNA-template.*

The MST signal (Fig. 2) changes stepwise with increasing template concentration. This corresponds to the changing ratio of unbound primer to primer-template complex and reflects the alteration of molecular properties upon binding. The fluorescence signals are normalized to the situation before heating and plotted against the template concentration. For moderate temperature gradients as used in MST experiments, the steady state concentration in the heat spot linearly reports the fraction bound. The data can thus be fitted to the quadratic solution of the law of mass action to obtain the dissociation constant.

The experiment was initially performed in PCR-buffer. To test the method's buffer independence, the interaction was also quantified in some rather exotic fluids like 50% espresso or camomile tea. In all cases, the binding affinity could still be derived from the thermophoretic signal (Fig. 3).

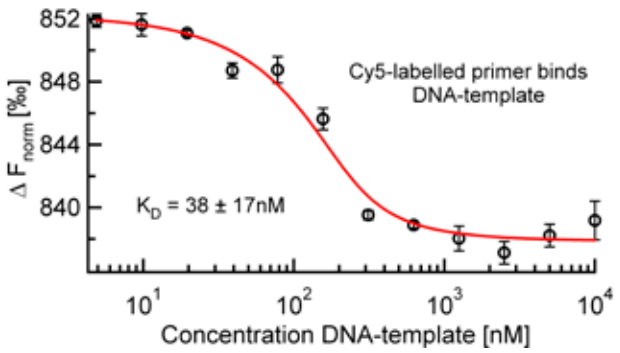

Fig. 3: *Primer-binding to a DNA-template. The thermophoretic depletion is plotted against the titrated template concentration and fitted to the law of mass action to determine the K_D. Triplicate measurements were performed in PCR-buffer with 50% camomile tea at room temperature; error bars represent standard deviation.*

In addition to these standard MST measurements with a fluorescence label, label-free MST measurements were performed utilizing the intrinsic UV-fluorescence of tryptophan residues in proteins. This exempts from tedious labeling procedures and clean-up steps. Thus, time and sample consumption is further reduced and the danger of altering the binding behavior by attaching fluorescence labels is averted. Label-free MST was employed to study different proteases. Proteases are enzymes that conduct proteolysis by hydrolysing the peptide bonds that connect the individual amino acids within a protein. Within the human body, these proteases have to be carefully regulated by specific protease inhibitors to avoid uncontrolled degradation of essential proteins. Thus, disregulation is associated with several diseases and commonly treated by the application of pharmaceutical protease inhibitors. The binding affinities of the proteases to their natural as well as to novel pharmaceutical inhibitors were thus investigated during the modules.

References:

1. S.A.I. Seidel, C.J. Wienken, S. Geissler, M. Jerabek-Willemsen, S. Duhr, A. Reiter, D. Trauner, D. Braun, P. Baaske: Label-Free Microscale Thermophoresis Discriminates Sites and Affinity of Protein-Ligand Binding, Angew. Chem. Int. Ed. Engl. 2012, 10656-10659.

2. S. Lippok, S.A.I. Seidel, S. Duhr, K. Uhland, H.-P. Holthoff, D. Jenne, D. Braun: Direct Detection of Antibody Concentration and Affinity in Human Serum using Microscale Thermophoresis, Anal. Chem. 2012, 84, 3523–3530.

3. S.A.I. Seidel et al.: Microscale Thermophoresis Quantifies Biomolecular Interactions under Previously Challenging Experimental Conditions, submitted to Methods.

Contact
Susanne Seidel
Braun Group
Department of Physics
LMU Munich
Amalienstr. 54
80799 München
Seidel.Susanne@physik.lmu.de

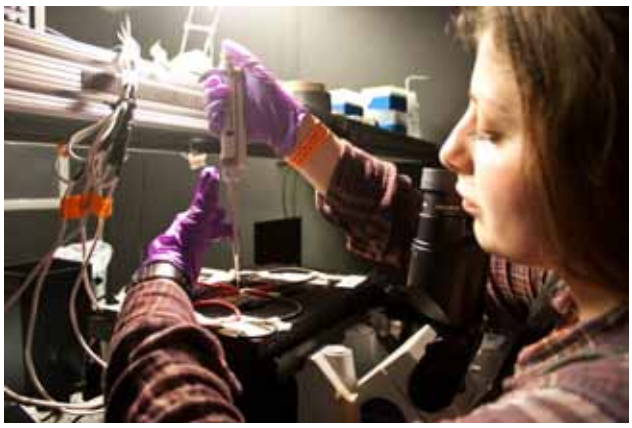

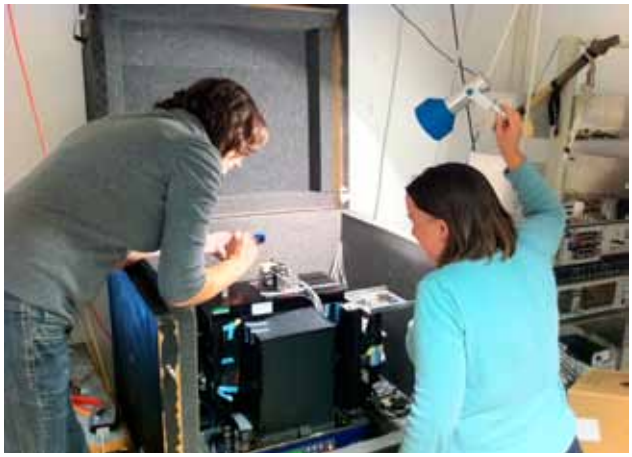

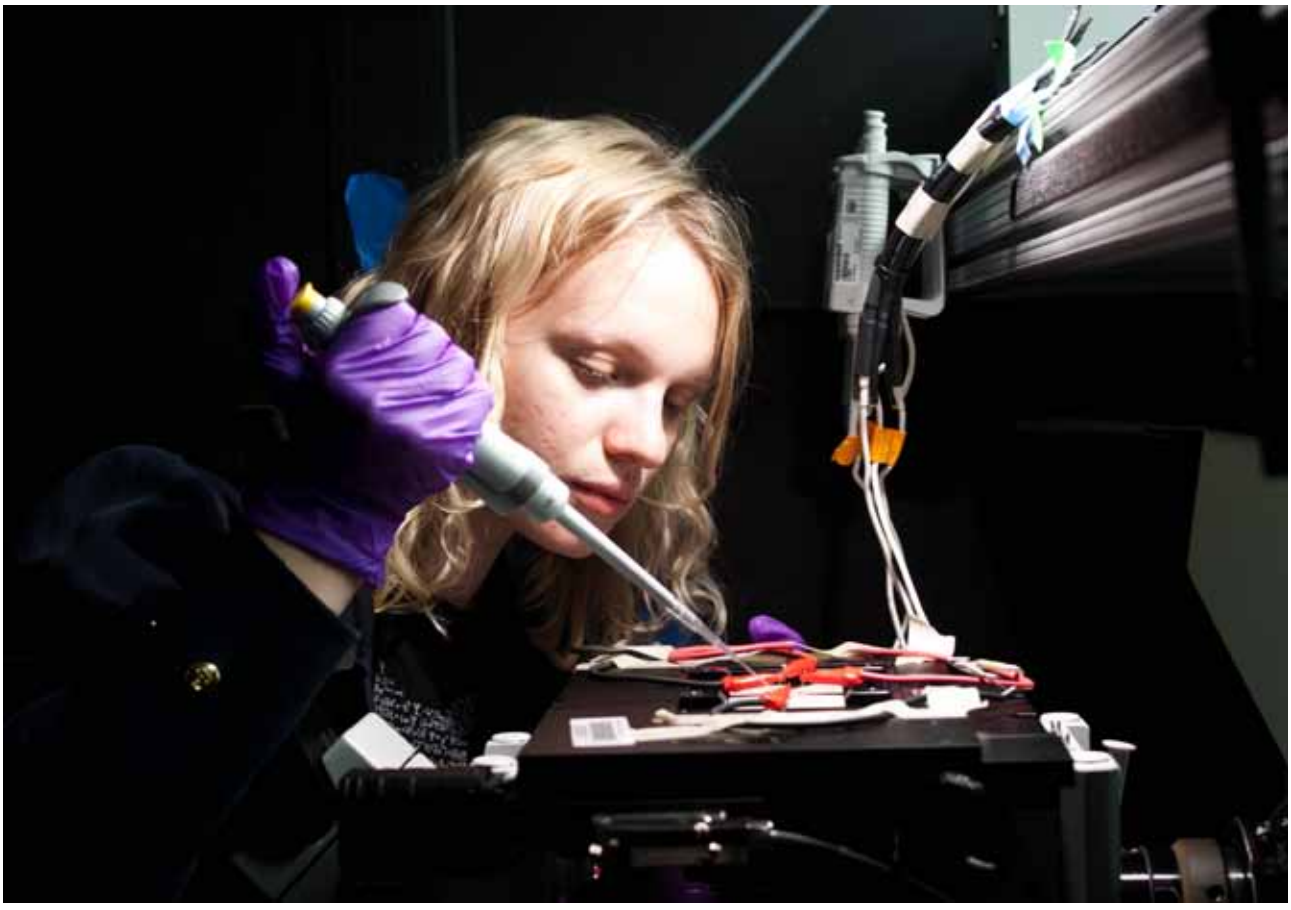

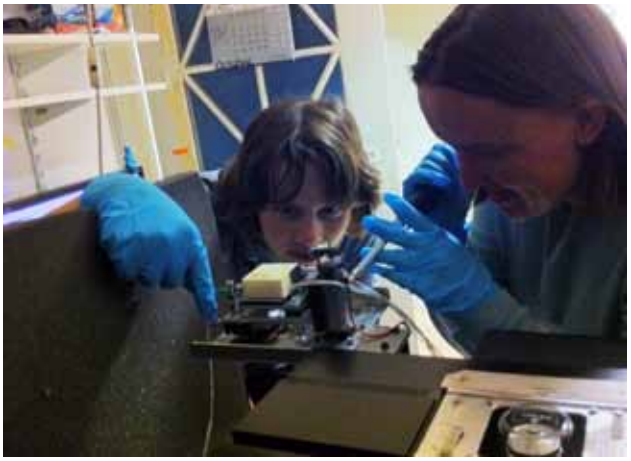

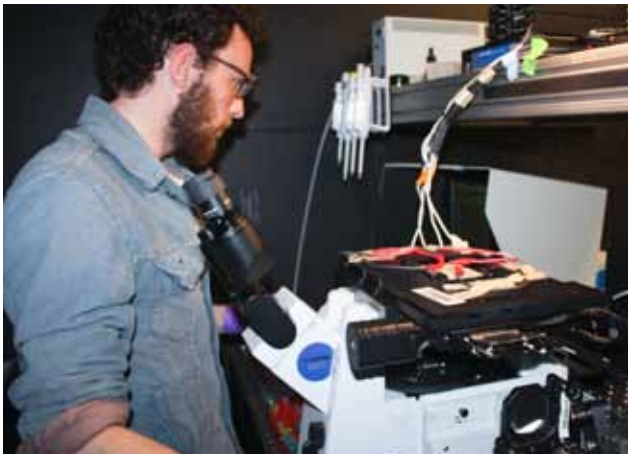

DI KANG

Fabricating Electrochemical Aptamer Based Cocaine Biosensor and Sensing Cocaine in Whole Blood

Recent years has seen the development of electrochemical biosensors comprising redox labeled oligonucleotide probes that are appended to an electrode surface. This biosensor uses a binding-induced structure-switching mechanism to detect nucleic acids, proteins and small molecules. An important advantage of this class of sensors is that their structure-switching signaling mechanism is reagentless and selective enough to deploy directly in complex sample matrices.

Electrochemical biosensor is a new class biosensor we developed since 2003, which is a folding based surface sensor. These sensors are comprised of an electrode modified with surface immobilized, redox-tagged DNA, have emerged as a promising new biosensor platform. The signal come from the electron transfer between the redox and gold surface. When the recgnition part in these sensors are aptamer DNA or RNA, we term this kind of sensor are Electrochemical, aptamer-based (E-AB) sensors, which predicated on the binding-induced folding of DNA or RNA aptamers and directed against targets ranging from proteins to small molecules to inorganic ions. Signal generation in the E-AB

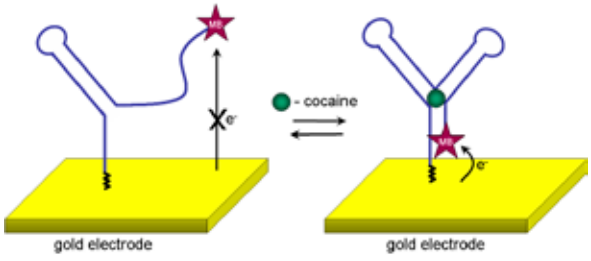

Fig. 1: *E-AB sensors rely on the specific binding induced folding of the aptamer in the presence of target.*

platform occurs when target binding alters the folding and flexibility of an electrode-bound aptamer. Because the sensing aptamer, and its attached redox tag, are strongly bonded to the interrogating electrode, E-AB sensors are reagentless and readily reusable. E-AB sensors are relatively insensitive to the nonspecific binding of interferants and perform well even when challenged directly in blood serum and whole blood.

In my lab training sessions, I take one of our E-AB sensing platform to show how dose our sensors work and teach the JNN student how to fabricate the basic E-ABsensor. The sensing target is cocaine.

Reagents and DNA Probes

Cocaine, 6-mercapto-1-hexanol (C6) and 10fold PBS buffer (Sigma Aldrich). For all cocaine sensor experiments, a 10× PBS buffer (Sigma Aldrich) was diluted 10-fold prior to use with ultrapure water (18 MΩ-cm Milli-Q Ultrapure Water Purification, Millipore, Billerica, MA) to 1 x PBS buffer (pH 7.0) buffered solution. The 5′-thiol-, 3′-methylene blue-modified DNA aptamer sequences (HPLC-purified, Biosearch Technologies, Inc. Novato, CA) were used as received without further purification. The cocaine sensor sequence employed was 5′-HS-$(CH_2)_6$-AGA CAA GGA AAA TCC TTC AAT GAA GTG GGT CG-$(CH_2)_7$-methylene blue-3′ as previously reported.

Sensor Fabrication

In brief, prior to sensor fabrication, gold disk electrodes (2 mm diameter, CH Instruments, Austin, TX) were cleaned both mechanically and electrochemically. Before use, cocaine sensor sequence DNA was reduced for 1 hr at room temperature in the dark in 10 mM TCEP. The relevant DNA probes were then immobilized onto freshly cleaned electrodes by incubating for 1 hr in 500 mM NaCl/10 mM potassium phosphate, pH 7 buffer with DNA concentration in 200 nM. The electrodes were then rinsed with distilled, deionized water, and incubated in 3 mM 6-mercapto-1-hexanol in 500 mM NaCl/10 mM potassium phosphate, pH 7 buffer for 30 min. Following this, the electrodes were rinsed in water water and stored in buffer for future use.

Electrochemical Measurements

Fabricated sensors were interrogated using square wave voltammetry (SWV) with a 50 mV amplitude signal at a frequency of 60 Hz, before and after a cocaine target step with increasing concentrations of the complementary target. To do this, the electrodes were first interrogated in a

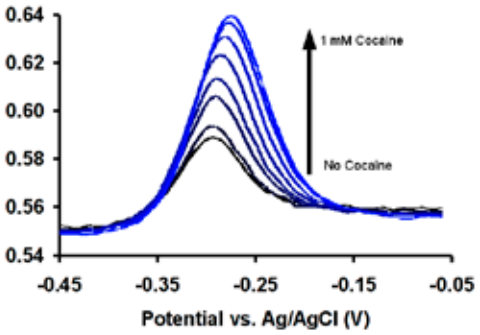

Fig. 2: *Typical SWV response of the E-AB sensor directed against cocaine. ACV peak current increases with increasing cocaine concentration for this signal-on sensor.*

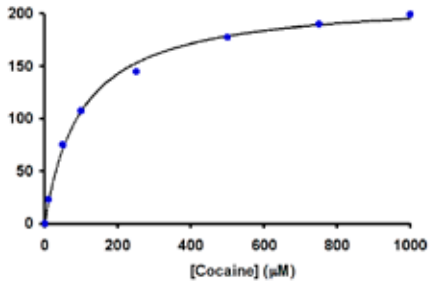

Fig. 3: *Binding curve showing E-AB signal gain (% signal change from peak current in absence of cocaine). The* k_d *= ~100 μM.*

pure buffer solution (background signal) 1 M NaCl/10 mM potassium phosphate, pH 7 and then titrite the cocaine, in every cocaine conenctration record the SWV output Signal gain was computed by the relative change in SWV peak currents with respect to background current.

Blood measurement is the same procedure, the only different is change the PBS buffer to a 30% Blood and PBS mixer.

Contact

Di Kang
Plaxco group
Department of Chemistry and Biochemistry
University of California Santa Barbara
Santa Barbara, CA 93106
dkang@chem.ucsb.edu

IDA PAVLICHENKO

Stimuli-Responsive Photonic Crystals for Sensing Applications

"Smart", stimuli-responsive photonic crystals (PCs) for label-free biological, chemical and physical sensing applications have gained recently a significant attention from various scientific communities, such as photonics, materials chemistry and biotechnology and represent a fast growing and prospective research field. A particular interest is attracted by simple yet promising and versatile one-dimensional PCs, christened Bragg stacks (BSs) shown in Figure 1 (a and b), namely the interference-based optical multilayer structures consisting of a periodic stack of layers of two different materials featuring high and low refractive indices (n), respectively.

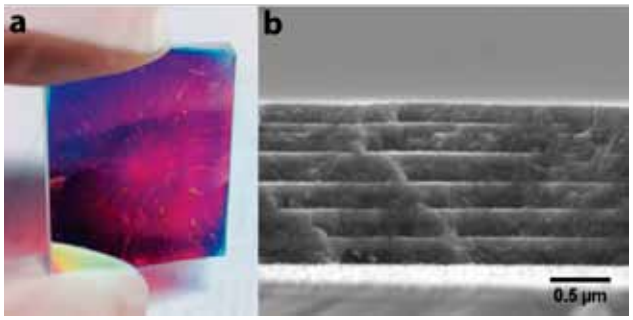

Fig. 1: *a) Photograph of SiO_2/TiO_2 nanoparticle-based BS fabricated via spin-coating method, b) The cross-sectional SEM image of the BS shown in Fig.1(a).*

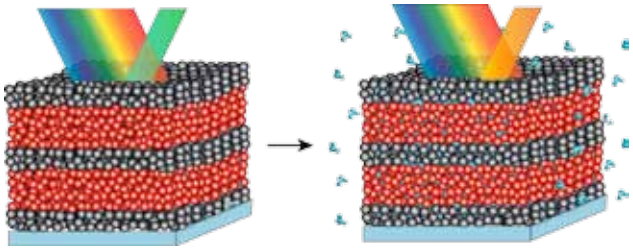

Fig. 2: *Schematic drawing of the Bragg stack before (left) and after (right) the exposure to the analyte of interest. The BS acts like an optical filter for the incident beam resulting in the observation of the photonic stop band.*

The sensing approach is based on the utilization of such PCs as tunable optical filters capable of dynamically changing their optical properties when in contact with an analyte of interest as presented schematically in Figure 2, or when exposed to external stimuli such as temperature, electric and magnetic fields, etc. Due to the periodicity of the dielectric lattice of the multilayer structure, which creates a periodic potential for photons in one dimension, the transmission or reflection spectra of the Bragg stack have the forbidden wavelength range for the photons with particular energies, called the photonic stop band. The position of the stop band can be modulated by varying the optical thickness (the product of RI and physical thickness) of the layers. One the prospective methods of the BS fabrication is the solution-processed deposition of nanoparticle suspensions. For example, the sol-gel method affords a relatively simple, fast and low-cost synthetic pathway to produce nanoparticles for the assembly of 1D PCs with high optical and structural quality by spin-, dip- or spray- coating. We propose photonic crystals designed in particular for vapor and temperature sensing based on the deposition of silica/titania multilayers via spi-coating. Herein, we investigate the response of the BS to the temperature changes, namely, we demonstrate the spectral shift of the photonic stop band for different nanoparticle-based BSs induced by the effective humidity-amplified thermo-optic effect, upon increasing temperature from 15 to 60 °C and show the response and recovery kinetics of the sol-gel processed multilayer systems during external changes in ambient humidity.

Contact

Ida Pavlichenko
Lotsch group
Max Planck Institute for Solid State Research and
Department of Chemistry
LMU Munich
Butenandtstrasse 5-13 (D)
81377 Munich
paich@cup.uni-muenchen.de

MICHAEL ISAACMAN

Clickable Amphiphilic Triblock Copolymers

Amphiphilic polymers have recently garnered much attention due to their potential use in drug delivery and other biomedical applications. A modular synthesis of these polymers is extremely desirable, because it offers precise individual block characterization and increased yields. This project aims for a modular synthesis of poly(oxazoline)–poly(siloxane)–poly(oxazoline) block copolymers using the copper-catalyzed azide–alkyne cycloaddition reaction . This approach uses copper nanoparticles as the catalyst, which are easily removed by filtration (Scheme 1). In addition to the synthesis, nanoscale vesicles were formed via solvent-directed self-assembly.

In the module we first calculated the appropriate amounts of hydrophilic poly(oxazoline) A-block and hydrophobic poly(siloxane) B-block required for the synthesis of ABA triblock copolymers. Each polymer was carefully massed and added to a round bottom flask with a stir bar. Chloroform was then transferred to the reaction vessel via an oven-dried syringe under an atmosphere of argon. The solution was degassed by bubbling argon through the solvent to remove oxygen, which can poison the catalyst. A catalytic amount of copper nanoparticles (~5 wt %) was then added and the reaction was heated to 80 oC for three hours. The sample was analyzed via proton Nuclear Magnetic Resonance, at which time it was determined the reaction was complete. The copper catalyst was removed via filtration and the solvent was concentrated to yield a pure product.

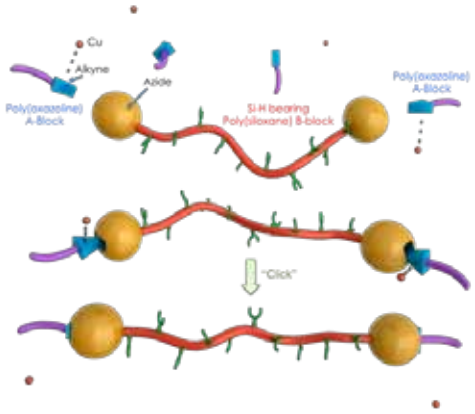

Fig. 1: *Schematic view of our click-based triblock copolymer synthesis. The A-blocks bear an alkyne terminal group, while the B-blocks are terminated with azides. The two blocks are clicked via a Copper catalyzed azide-alkyne click reaction. The blocks can be further derivatized via a hydrosilylation reaction.*

Vesicles were then formed by dissolving the polymer in a minimal amount of ethanol, followed by addition into water. The resulting mixture cleared after 30 minutes of stirring, indicating vesicle formation. The solution was filtered through a 250 nm syringe filter to remove any contaminates. A small sample was removed and the hydrodynamic radius of the vesicles was analyzed using Dynamic Light Scattering (DLS), which demonstrated a radius of ~40 nm.

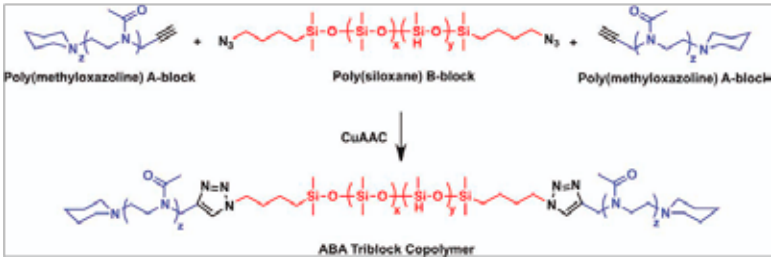

Fig. 2: *Synthesis of ABA triblock copolymer from alkyne-functionalized poly(oxazoline) A-block and bis-azide poly(siloxane) B-block homopolymers via copper-catalyzed alkyne-azide cycloaddition (CuAAC) click reaction.*

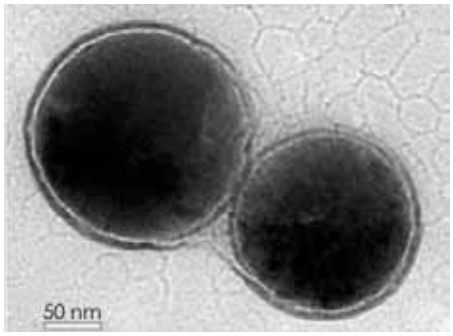

Fig. 3: *Transmission electron micrograph of ABA triblock copolymers.*

Contact

Michael Isaacman
Theogarajan group
Department of Chemistry and Biochemistry
UC Santa Barbara
Santa Barbara, CA 93106
misaacman@chem.ucsb.edu

PAUL ZAKREVSKY

Design and Assembly of RNA Nanoparticles

Natural RNA molecules assume complex three-dimensional (3-D) structures through formation of a variety of base pairing interactions. By interacting through both through Watson-Crick and non-canonical base pairings, RNA can form a vast array of local structural folds (1). Additionally, long-range intra- and inter-molecular base pairs allow for the formation of compact structures and supra-molecular assemblies (2,3).

RNA motifs are the structural building blocks that enter into the composition of large, complex structures of RNA molecules. These motifs are encoded by local sequence signatures and result in recurrent, defined geometries of the RNA backbone. Motifs of greater complexity and size can be built from simpler smaller ones in a hierarchical way, to result in complex 3-D folds (4). RNA architectonics is the concept whereby RNA motifs are spliced out of their natural molecular context and combined to form novel, pre-defined RNA structures (5). The large library of structural motifs yields an abundance of options for defining geometries and interactions for the rational design of novel RNA particles.

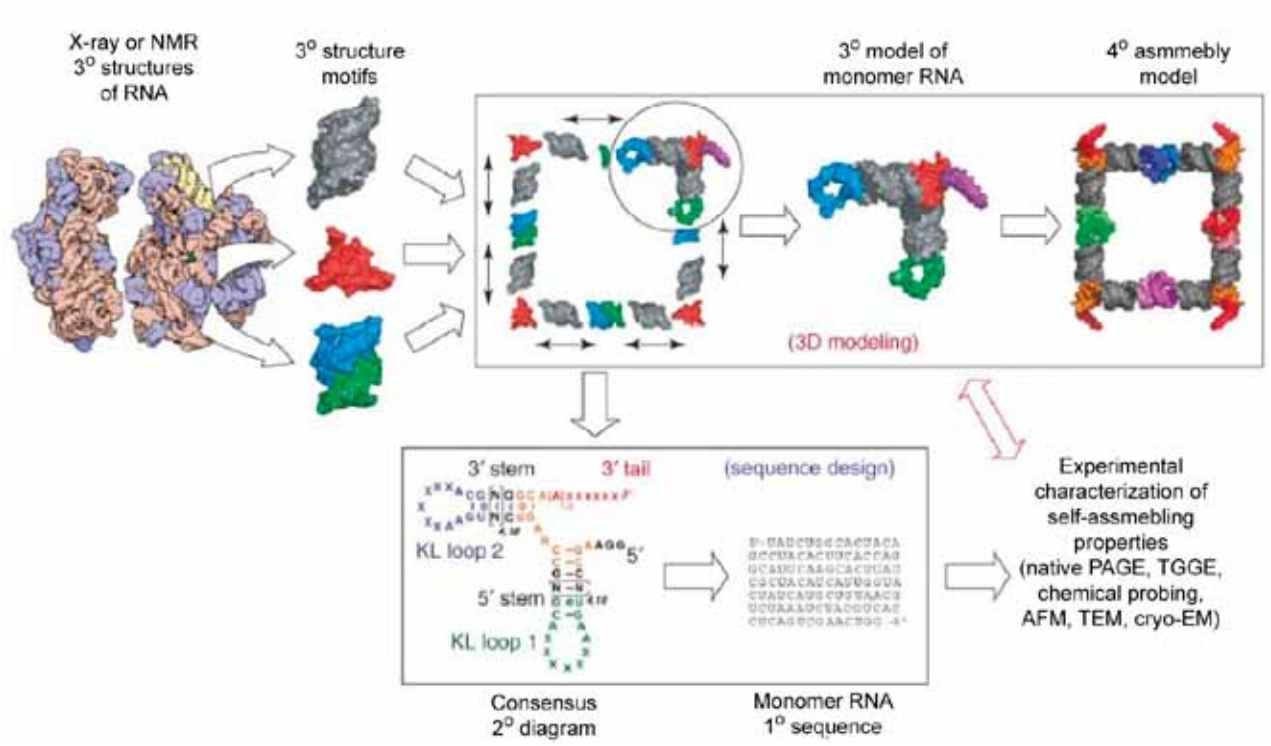

Fig. 1: *Scheme for RNA particle generation using the RNA architectonics design approach. Tertiary structural motifs are use to generate a 3-dimentional computer model of the desired RNA assembly. The model is then used to produce a secondary structure diagram of each monomer unit, from which a primary nucleotide sequence can be designed.*

In this teaching module, students were introduced to the architectonics approach for RNA design, beginning with structure and sequence optimization and working towards RNA assembly and characterization.

The module began with a discussion regarding the initial design phases required to produce an RNA assembly from multiple monomer units. Students were then introduced to sequence optimization methods for designing RNA monomers. It is of critical importance to ensure that each RNA sequence folds in vitro as it was designed to fold in silico. Students were shown ways to find the most thermodynamically stable secondary structure of a given RNA sequence, how to avoid folding traps, and how to design RNA monomer sequences able to fold and assemble during transcription (6). This is a nice alternative to methods involving

RNA transcription followed by the purification of each RNA monomer by denaturing polyacrylamide gel electrophoresis before RNA assembly *in vitro*. Following the discussion on sequence optimization, students were given the opportunity to generate 3-D computer models of hexameric RNA nanorings. Students learned how to search and splice out structural motifs of interest from existing x-ray or NMR RNA structures. With the use of DeepView/Swiss-PdbViewer, students were able to create their own 3-D model of an RNA nanoring. These models could then be used to establish the length of helical regions for optimization of monomer geometry and the positioning of intermolecular interactions.

The final activity of the module gave students a chance to assemble RNA nanorings composed of various numbers of unique monomer units through selective kissing-loop interactions (7). In addition to forming closed RNA ring assemblies, student also assembled appropriate RNA molecular controls. They analyzed their assemblies by native PAGE.

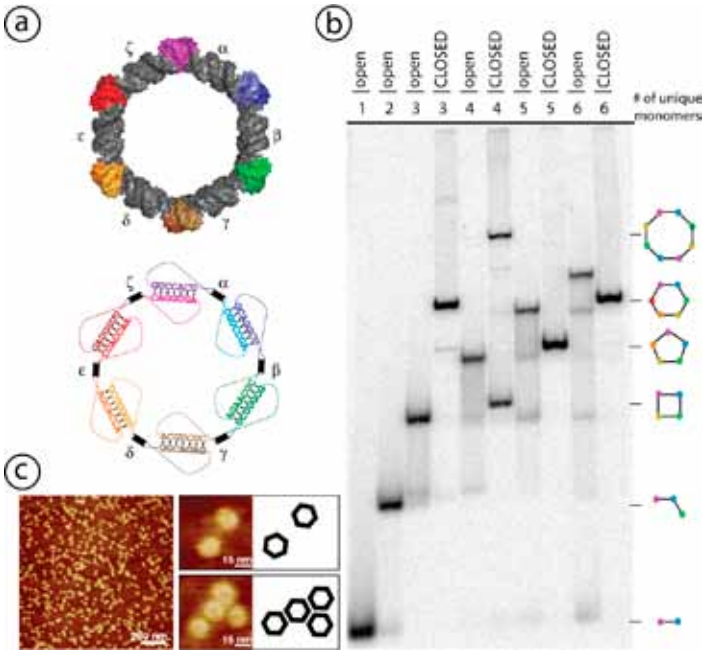

Fig. 2: *Assembly of RNA nanorings. (a) 3-dimensional computer model (top) and secondary structure diagram of heximeric nanorings composed of six monomer units. (b) Native PAGE analysis of closed rings and open chain control assemblies composed of various numbers of unique monomer units. (c) AFM images of RNA nanorings.*

References:

1. Leontis, B. and Westhof E. (2003) Curr. Opin. Struct. Biol. 13: 300-308.
2. Noller, H. (2005) Science. 309: 1508-1514.
3. Severcan, I. et al. (2010) Nature Chem. 2: 772-779.
4. Chworos, A. et al. (2004) Science. 306: 2068-2072.
5. Jaeger, L. and Chworos, A. (2006) Curr. Opin. Struct. Biol. 16: 531-543.
6. Afonin, K. et al. (2012) Nano Lett. 12: 5192-5195.
7. Grabow, W. et al. (2011) Nano Lett. 11: 878-887.

Contact
Paul Zakrevsky
Jaeger group
Department of Chemistry and Biochemistry
University of California, Santa Barbara
Santa Barbara, CA 93106 USA
pzakrevsky@chem.ucsb.edu

CHRIS CARACH

Fabrication of Organic Solar Cells

Organic Photovoltaics (OPVs) are widely studied for their potential use as a low-cost source of electrical energy. Polymer photovoltaics are an important class of OPVs that typically employ a thiophene-based light-absorbing polymer and a C60 (buckyball) sensitizer to create free charge carriers. The polythiophene chains and buckyballs have to be properly mixed at the nanometer length scale for optimal charge extraction. In the Gordon Group at UCSB, we employ both far-field (absorbance, PL, Raman) and confocal/near-field optical spectroscopy to study the nanoscale morphology of these OPVs.

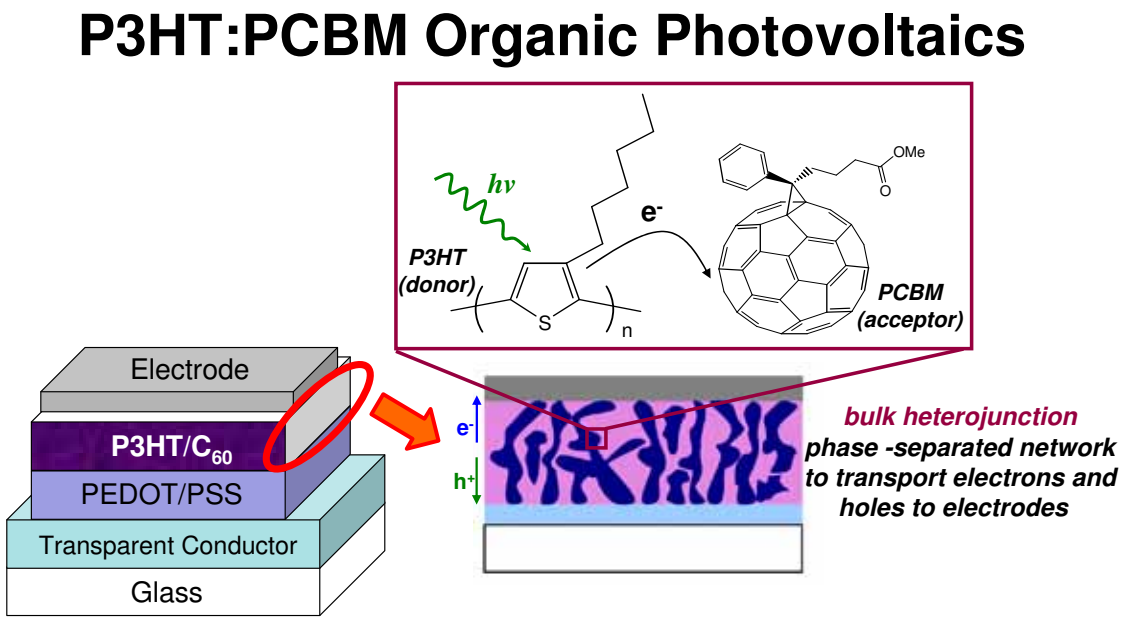

Fig. 1: *Schematic of an organic ("plastic" or polymeric, in this case) photovoltaic device, along with a zoom-in of the "bulk heterojunction" architecture of the light-absorbing layer.*

However, another aspect of our research is to correlate the morphology to device performance, so we also make and test solar cells. This, essentially, was the JNN lab project. Figure 2 shows the step-by-step OPV fabrication process, in which the JNN students participated fully. It involves some standard thin-film processing operations (e.g., spin-coating, thermal evaporation) with the twist that much of the equipment was home-built (from the RF plasma cleaner to the automated I-V test station), offering a somewhat unique hands-on experience.

After fabricating their own solar cell (actually four solar cells, to hedge against any defective devices), JNN students got to test the photovoltaic performance. This involved making electrical contact in the test station, shining in some light, sweeping the voltage and measuring the current. The I-V curves of the best solar cells of each participant are displayed in Figure 3. Florian takes home 1st prize, as his solar cell exhibited the highest open-circuit voltage, short-circuit current, and power output. The team of Svenja and Johanna were right behind, along with Markus, whose solar cell gets the special award for highest fill factor (to speak loosely and forego the technical definition, highest fill factor = "nicest-looking" I-V curve). For each participant, their fourth and final solar cell performed slightly better than any of the first three, casting anecdotal doubt on the English proverb, "third time's a charm."

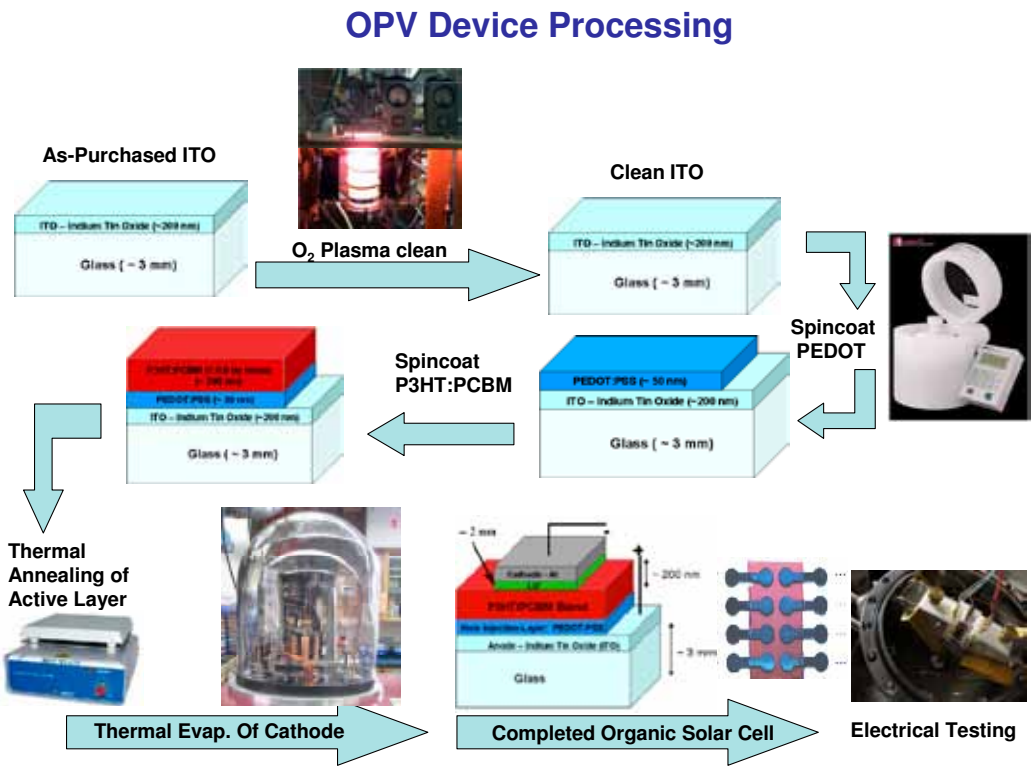

Fig. 2: *How to make an organic photovoltaic device. The steps of the process are exactly as done by the JNN participants, and the photos are of the actual equipment in the Gordon Lab.*

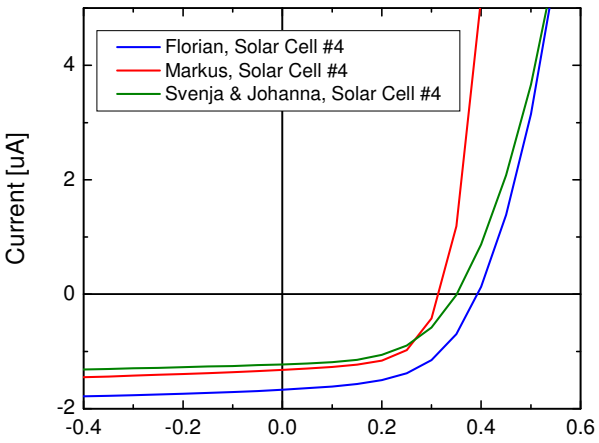

Fig. 3: *I-V (current-voltage) characteristics of the completed OPV devices under blackbody illumination (~1/2 sun).*

Contact

Chris Carach
Gordon group
Dept. of Chemical Engineering
Univ. of California, Santa Barbara
Santa Barbara, CA 93106-5080
cac01@umail.ucsb.edu

KIMBERLY WEIRICH

Forming Lipid Tubules from Supported Lipid Bilayers by Thermal Stress

Biological Membranes spatially transform in response to environmental stresses such as area expansion, osmotic pressure, and protein insertion. It is not understood how adhesion to a support, such as a surface or cytoskeletal network, influences this remodeling. Supported lipid bilayer (SLB) is a model membrane system in which a bilayer is adsorbed to a solid (glass) support. We use SLB to quantitatively investigate fluid bilayer transformations from planar to tubular morphologies.

In this JNN module, students learned the essentials of working with lipids and supported lipid bilayers. We learned to prepare supported bilayers. We first extruded a lipid suspension into unilamellar vesicles. We then adsorbed the vesicles to clean glass to form a high quality, supported lipid bilayer. As vesicles adsorbed, we watched the formation of supported lipid bilayer using video fluorescence microscopy. Finally, we explored the effects of thermal stress on supported bilayer transformation to tubular morphology. Taking advantage of the area expansion mismatch between the bilayer and the glass, we formed lipid worms by increasing the temperature of the supported lipid bilayer by a few degrees. After imaging the worms, modules experimented based on their interests. In one module, we used osmotic stress to probe worm morphology. Decreasing the ionic strength of the surrounding solution caused the worms to swell into resolvable tubules, while increasing the ionic strength caused rapid collapse of the tubules. In another module, we further explored the effects of thermal stress on worm stability and supported bilayer integrity. Decreasing the temperature after worm formation caused holes to form in the lipid bilayer.

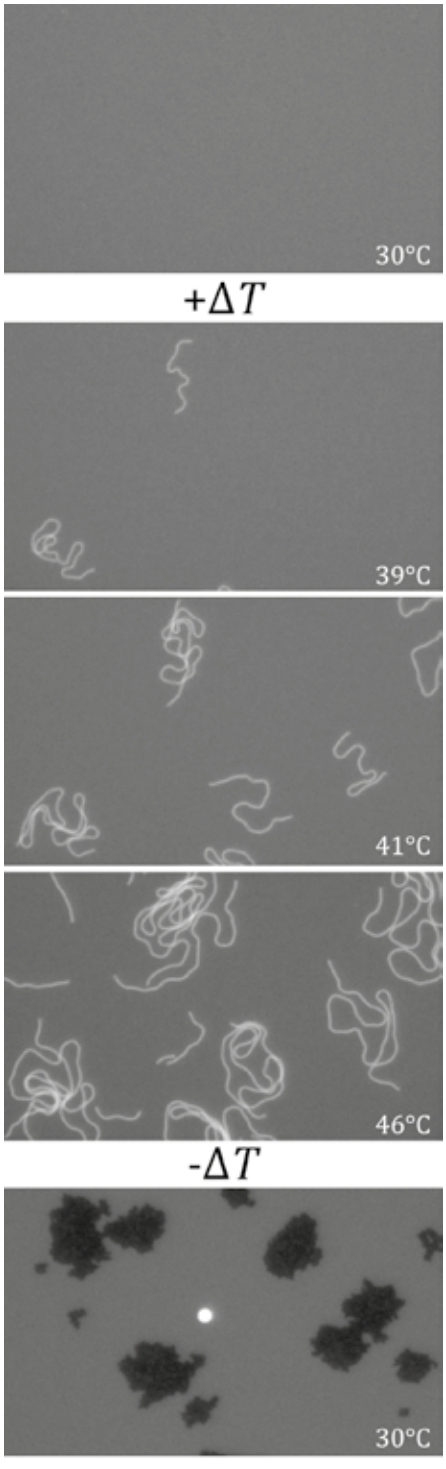

Fig. 1: *Lipid worms extrude from an initially uniform supported lipid bilayer upon heating. Fluorescence micrograph snapshots taken far from the boundaries of a cm-sized SLB during a continuous temperature ramp (~0.8°C/min).*

Contact

Kimberly Weirich
Fygenson group
Biomolecular Science and Engineering
University of California
Santa Barbara, California 93106
kweirich@physics.ucsb.edu

COLIN FELLOWS

Interfacial Microrheology of Phospholipid Monolayers

Lung surfactant (LS) is a complex mixture of lipids and proteins that forms a molecularly-thin film at the air-alveolar interface. Proper surfactant function is essential for respiration to reduce the surface tension at this interface and thus significantly reduce the work required for breathing. A deficiency in the LS system can lead to serious problems in the respiratory process. Current LS replacement therapies used to treat the related diseases vary significantly in composition. To alleviate various problems associated with animal-derived LS replacement therapies, it is desirable to rationally design and optimize effective synthetic replacements. In particular, we are interested in the rheological properties of the surfactant film. During exhalation, a large surface tension gradient develops between the alveoli and the airways which seeks to drive fluid out of the alveolar spaces. We hypothesize that a high surface shear viscosity, elasticity, and yield stress of the LS film prevents the flow of surfactant out of the lungs. We seek to find connections between monolayer structure, composition, and physical properties in order to gain further insight into the behavior of model LS systems.

In order to measure the surface dynamic properties, we place micron-scale magnetic disks within the surfactant monolayer at the air-water interface. An oscillatory magnetic field is applied to the disk, and the angular orientation of the disk is tracked via bright-field microscopy. With the known applied stress and the measured strain, we obtain the surface viscoelastic shear properties of the monolayer. Simultaneously, the phase behavior of the monolayer is studied by monitoring the surface pressure and visualizing the domain structure via epifluorescence microscopy.

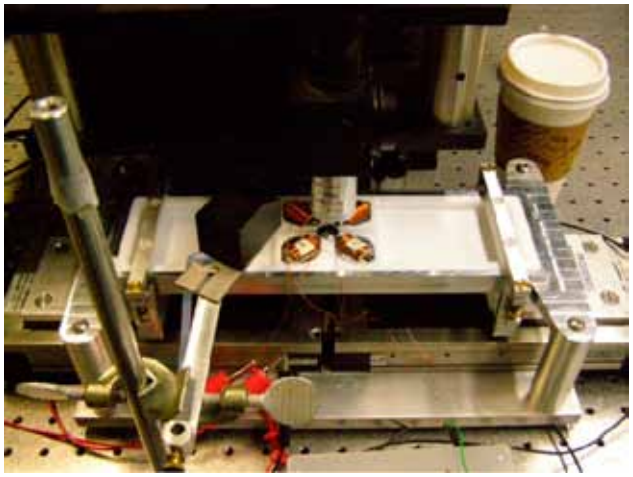

Fig. 1: *Experimental setup – Langmuir trough with electromagnets to induce torque on the magnetic microdisks; simultaneous visualization with epifluorescence and bright-field microscopy.*

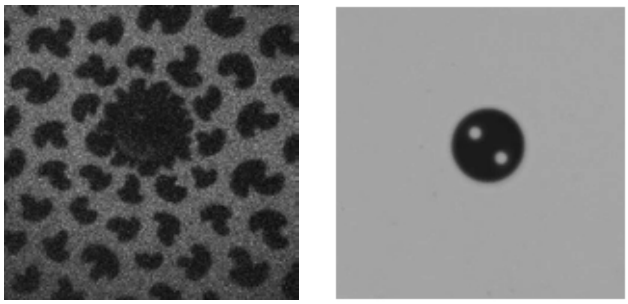

Fig. 2: *Visualization of a magnetic disk embedded within a phospholipid monolayer (80/20mol% DPPC/POPG at 12 mN/m; fluorescent contrast due to 0.2% Texas Red DHPE) by fluorescence microscopy (left) and bright-field microscopy (right). Disk diameter is 20 μm.*

Contact

Colin Fellows
Squires group
Department Chemical Engineering
University of California
Santa Barbara, California 93106
cfellows@umail.ucsb.edu

MEHRIJE FERIZI

Transcript-Therapy – a Novel Therapeutic Approach for Disease Treatment

In-vitro transfection studies with SNIM-RNA using magnetofection

Very recently, a novel therapeutic approach for the treatment of acquired and inherited diseases been developed, so-called transcript therapy. Here, messenger RNA is delivered instead of its counterpart DNA into the target cells. However, scientists have to conquer two major hurdles. First, due to the short half-life of mRNA, repeated dosing would be necessary to achieve the desired therapeutic effect. Therefore, attempts have been made to optimize mRNA stability and its translational efficiency. Until now, several strategies have been developed and have been successful in increasing mRNA stability and reduce the immunogenic response triggered by externally administered mRNA. One such promising strategy is the inclusion of chemically modified nucleotides in mRNA to generate stabilized non-immunogenic messenger RNAs (SNIM-RNA). Secondly, the choice of an optimal delivery system, which improves transfection efficiency and the SNIM-RNA expression kinetics, is also of vital importance. One such promising nucleic acid delivery technology is magnetofection. The principle of magnetofection is based on the association of nucleic acids with magnetic nanoparticles (see fig.1) forming a magnetic vector. These magnetic vectors can than be directly guided towards target cells by applying an external magnetic field. Focus of this project is the combination and investigation of these new technologies for SNIM-RNA transfection into cells.

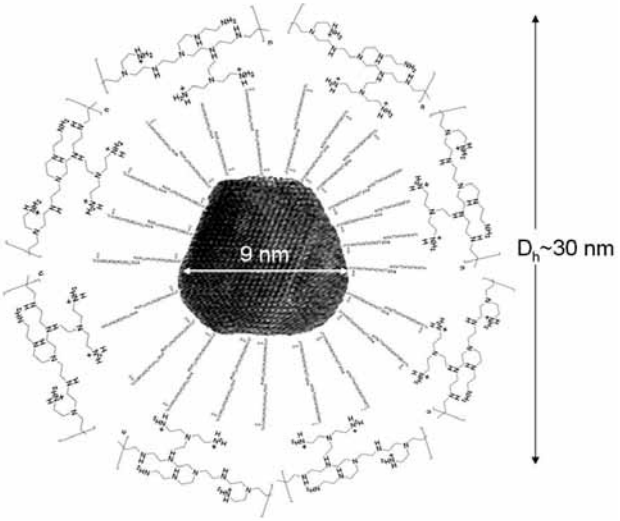

Fig. 1: *Iron oxide magnetic nanoparticles for gene delivery: The iron oxide core has a size of 9nm and is coated with branched PEI. The coating of the iron oxide stabilizes the particle and enables a better binding to the nucleic acid. The total size of these magnetic particles is approximately 30nm.*

For this purpose an in-vitro transfection study was performed by using different complexes, such as SNIM-RNA with magnetic nanoparticles (magnetic duplexes), cationic lipids combined with SNIM-RNA (lipoplexes) and magnetic duplexes combined with a cationic lipid (magnetic triplexes) to transfect the cells with and without magnetic field. The students of this module first learned to produce modified messenger RNA "SNIM RNAs" coding for a reporter gene, the Metridia luciferase. The production of SNIM-RNA was simply done by in-vitro transcription reaction in a reaction tube without necessity of living cells. For this reaction linearized template DNA, which contains the sequence of the reporter gene, as well as the T7 polymerase with the ideal buffer conditions and the ribonucleotides, the natural and modified ones, were needed. The in-vitro transcription reaction is an easy method to synthesise mRNA for the daily

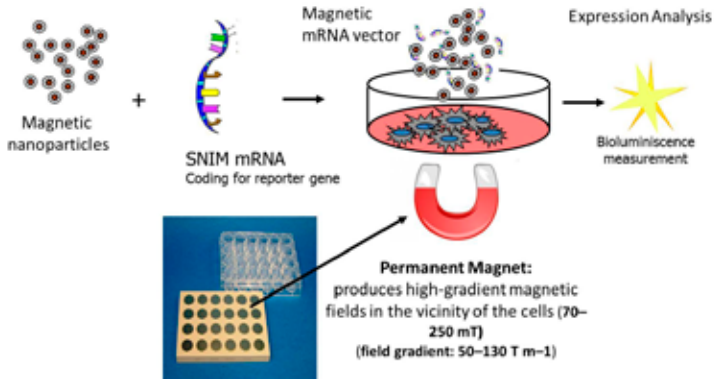

Fig. 2: *Experimental Setup - Magnetofection: Magnetic vectors are formed by mixing magnetic nanoparticles with SNIM RNA (magnetic duplexes) and are added onto cells in culture. The cell culture plate is positioned on a magentic plate for 30 minutes. Under magentic field magentic vectors are quickly sedimented on the cells to be transfected. By bioluminiscence measurement the expression of the nucleic acid can be detected.*

lab use. After synthesis of SNIM-RNA the students conducted the transfection of eukaryotic cells with SNIM-RNA using magnetofection. Here the different complexes were first prepared by pipetting the corresponding components together and incubate them for a couple of minutes at room temperature. The ready-to use complexes were added onto the cells and a magnetic field was applied for 30 minutes to allow a synchronized sedimentation of the complexes. Afterwards the transfected cells were put back in the incubator at 37°C. Once the transfected cells produce the reporter protein, it is secreted into the supernatant and can be easily detected by bioluminescence measurement (see fig.2). For this measurement a part of the supernatant is mixed with the substrate coelenterazine. During this biochemical reaction light is emitted and can be detected immediately. This kind of measurements enables to gain an insight into the expression kinetics profile of the SNIM-RNAs over several days. However, due to time limitation measurements could not be completed for every single day. Nevertheless, the exchange-students could observe that magnetic triplexes, SNIM-RNA combined with magnetic nanoparticles and cationic lipid, compared to magnetic duplexes showed an improved expression under magnetic force (see fig.3).

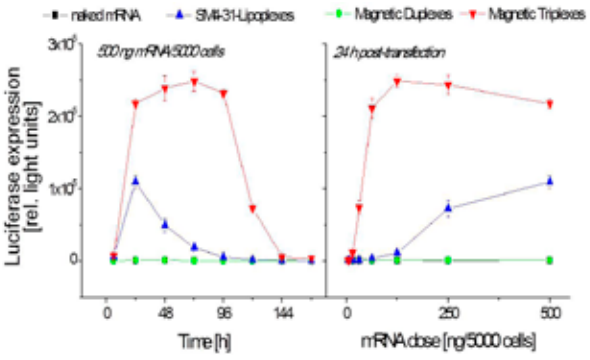

Fig. 3: *Reporter expression after transfection of cells with SNIM-RNA coding for Metridia luciferase using naked mRNA, cationic lipid/ SNIM-RNA lipoplexes, MNP (magnetic nanoparticles)/SNIM-RNA duplexes and with MNP/ cationic lipid/SNIM-RNA triplexes, 96-well magnetic plate was applied for 30 min after adding the complexes. Bioluminiscence measured in supernatant after adding coelenterazine and is plotted as a function of time (left) and mRNA dose (right).*

Contact

Mehrije Ferizi
Plank group
Institute of Experimental Oncology and Therapy Research
Technical University Munich
Ismaningerstraße 22
81675 Munich
mehrije.ferizi@lrz.tum.de

JOHN BEREZNEY

Magnetic Tweezers Measure Translocation of Helicase Motors on DNA

Magnetic tweezers are able to directly observe the mechanical properties of double-stranded DNA (dsDNA). Here, we use the magnetic tweezers to examine the procession of the replicative helicase, gp41, as it unravels a single molecule of dsDNA. We measure both its unwinding rate as well as its single-stranded DNA (ssDNA) procession rate.

This module allowed students to use magnetic tweezers to study the interaction of proteins with DNA. While holding DNA hairpins under tension within a flow cell using the magnetic tweezers, students added helicase proteins and ATP and then observed the proteins' procession along individual DNA molecules. The extensions of the molecules over time were then analyzed to quantify two features of helicase/DNA interactions: the dsDNA unwinding rate and the ssDNA procession rate.

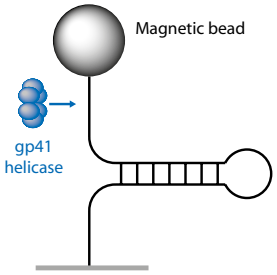

Fig. 1: *Sketch of 389-bp hairpin immobilized between coverglass and magnetic bead. Gp41 helicase loads onto the ssDNA handle and processes in the 5' to 3' direction.*

To measure the procession of single hexamers of gp41 along DNA, we used a tethered hairpin assay. Students prepared flow cells in which 389-bp DNA hairpins with single-stranded DNA handles were immobilized by one terminus to an anti-digoxigenin coated surface and by the opposite terminus to a streptavidin coated superparamagnetic bead (Fig. 1). Using the magnetic tweezers, students applied force to the hairpin, measured the hairpin's extension and observed the hairpin's critical mechanical unfolding force. Below this force, the hairpin is in a stable, collapsed configuration while above this force, the hairpin is destabilized and takes on a longer, open conformation.

Contact

John Berezney
Saleh group
Department of Materials
University of California
Santa Barbara
Santa Barbara, CA 93106-5050
berezney@umail.ucsb.edu

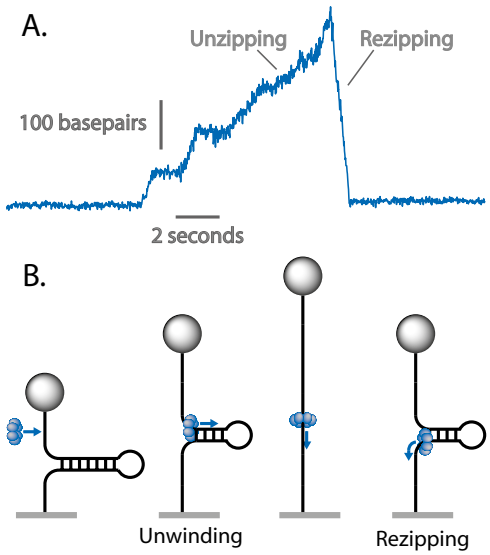

Fig. 2: A. *Representative data from a helicase unwinding event.* ***B.*** *Cartoon of hairpin action. The helicase loads onto the ssDNA. As it unwinds the hairpin, the extension increases. Once the helicase passes the hairpin loop, the DNA reanneals behind it and the extension decreases.*

When students added gp41 helicase and ATP to flow cells containing stable, folded hairpins, changes in the hairpin extension were observed; there were steady increases in the bead height up to the full extension of the hairpin which were followed by a faster decrease back to the extension corresponding to the fully folded hairpin conformation (Fig. 2). These were observations of helicase translocation along the hairpin structure. First, the helicase unwound the hairpin, causing the hairpin to open; this was observed through the increase in extension. Second, the helicase traveled along the remaining ssDNA, allowing the hairpin structure to reanneal behind it; this was observed through the decrease in extension. By analyzing this data, the students quantified the unwinding rate of gp41 at 8 pN to be 66 bp/s and the ssDNA translocation rate to be 449 bp/s.

Reference:

1. N. Ribeck, D.L. Kaplan, I. Bruck, I. and O.A. Saleh. Biophysical Journal 99, 2170 (2010).

KAMILA KLAMECKA

Single-Molecule Cut&Paste

Single-Molecule Cut&Paste allows for directed transfer of individual biomolecules between different areas on a glass surface. The precision at which the molecules are deposited is limited by the length of the polymeric anchors and is presently in the 10 nm range. The technique is based on a custom-built hybrid of Total Internal Reflection Fluorescence Microscope and Atomic Force Microscope (TIRFM-AFM). AFM provides the nanometer-scale precision while TIRFM allows for visualization of the printed pattern.

Precise manipulation with biomolecules on the single-molecule level is an inevitable necessity in the miniaturization of biochemical systems. Single-Molecule Cut&Paste is meant to serve as a tool for a large range of applications, providing deeper insight into enzyme cascades and networks.

Fig. 1: *"JNN 2012" pattern assembled during the JNN lab class by Single-Molecule Cut & Paste from approximately 700 DNA oligonucleotides labeled with Atto647N fluorophores.*

Here, we transferred single-stranded DNA oligonucleotides. The mechanism of the molecules transfer was based on DNA complementarity. Transfer molecules were picked up from the region referred to as depot and then moved to the target area. Immobilization was accomplished through complementary DNA hybridization. Both depot and target were functionalized with covalently linked to the surface single-stranded DNA oligonucleotides. These were complementary to part of the transfer DNA. The remaining overhang of the transfer DNA was in turn complementary to a single strand at the AFM cantilever. Transfer DNA was labeled with a fluorophore so after successful pattern assembly, it could be visualized. Surface functionalization was done using microfluidic channels separated about 20 micrometers from each other.

Target and depot DNA had the same sequence but differed in anchoring geometry – one was fixed to the surface by its 3' and the other by 5' end. This resulted in substantial difference in rupture forces under external load applied during pick-up and deposition of the transfer molecule. In one case – the "zipper" mode – the DNA duplex was being torn apart by pulling on the side where it was anchored. The base-pairing was destroyed stepwise (one-by-one hydrogen bond) and the force needed to separate the two strands was independent of the length of the duplex. In the other, "shear" geometry, the duplex was pulled on the end opposite of the attachment to surface. This way all the hydrogen bonds between the bases were attacked at once. In the shear mode the force is much higher and it scales up with the length of the double-stranded fragment.

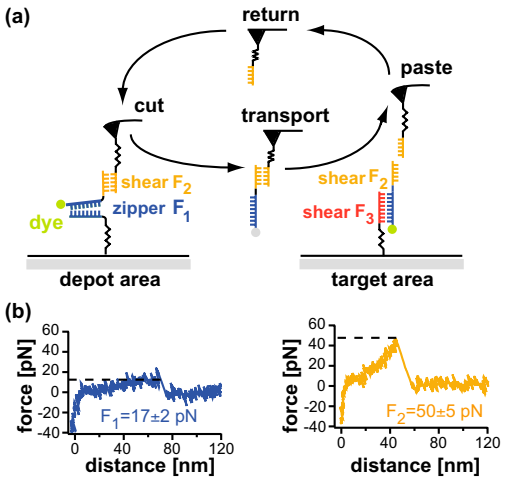

Fig. 2: *Single-Molecule Cut&Paste of DNA oligonucleotides; a: schematic representation of a single cycle, b: force traces recorded for each unbinding event at depot and target; fig. from Gumpp et al., Rev Sci Letters 2009.*

Force hierarchy – crucial for successful multiple cycles of DNA pick-up and deposition – was realized through different mechanical stability of the so-called "zipper" and "shear" geometries of the DNA sequence. The binding of the molecule to the handle needs to be stronger than to the depot area and at the same time weaker than that at the target area.

Reference:

1. Kufer et al.: Single-Molecule Cut-and-Paste Surface Assembly; Science 319 (5863) pp. 594-596 (2008)

Contact
Kamila Klamecka
Gaub group
Physics Departement
LMU Munich
Amalienstr. 54
80799 München
klamecka@gmail.com

FLORIAN STROBL

Influence of Nanoparticles on Morphological Transitions of Lipid Membranes

Lipid bilayers are the basic structure of biological membranes. Their physical properties are strongly dependent on their thermodynamic state which can be altered by different environmental influences. In this module students could see how phase transitions can drastically change the morphology of lipid membranes and how nanoparticles influence this transition behavior.

Artificial lipid bilayer membranes are studied since many years by different techniques to gain deeper insight into fundamental phenomena with high relevance for living cells. Both, the phase state of lipids [1] and membrane particle interaction [2] are considered to be of high importance in biological processes like cell trafficking and signaling.
As a simple model for cell membranes fluorescent labeled giant unilamellar vesicles (GUVs) with a lipid composition of DMPC/DPPC(1:1) where produced by electroswelling [3] in a 0.2M sucrose solution and observed in a temperature regulated chamber filled with an equi-osmotic glucose solution. The chamber bottom was sealed with glass slides which had to be spin coated with a thin layer of Teflon® AF in advance to prevent adhesion of vesicles.
First the morphological behavior of vesicles in pure glucose solution was observed during a temperature ramp through their gel to fluid phase transition temperature and the phase diagram of lipid membranes was discussed. Thereafter the experiment was repeated in the presence of silica nanoparticles. A comparison of both cases can be seen in figure 1.

We could observe that the particles enforce the development of internal particle-loaded buds. Depending on the particle species a distinct typical bud radius is stabilized (fig. 2).

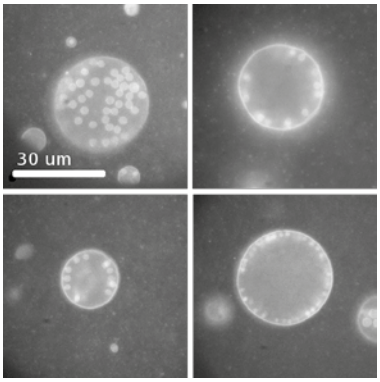

Fig. 2: *Depending on the used nanoparticle type (here: Si-particles with 120nm diameter and weakly neagtive ζ-Potential, not visible) a distinct typical bud size is enforced which depends on the specific properties of the individual vesicle. Within one vesicle the size distribution is astonishingly sharp.*

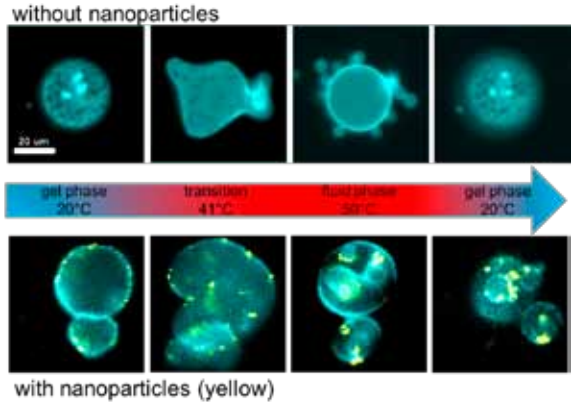

Fig. 1: *Phase transition triggered endocytosis-like behavior. Top: Vesicles usually show extravesicular budding when undergoing a transition from gel to fluid phase in the given environment. Bottom: The adhesion of particles (yellow) makes intravesicular budding more favorable. After a full temperature cycle almost all particles are internalized into internal buds.*

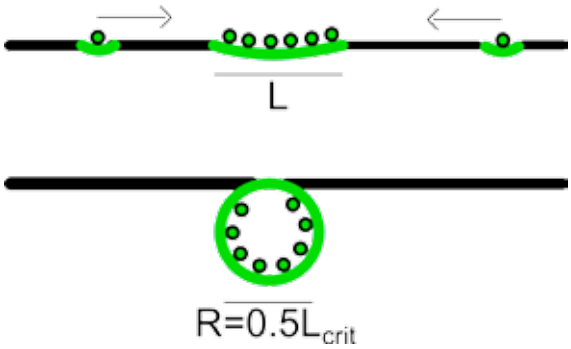

Fig. 3: *Possible explanation for the observed behavior: domain induced budding. Particle loaded domains grow up to a critical size L_{crit} where a domain with low curvature transforms into a spherical bud.*

Possible theoretical explanations and the relevance of these observations for biological systems were discussed. On the one hand particle contact can change the thermodynamic state of lipid membranes [4] and phase state related budding events potentially play a crucial role in cellular particle uptake. On the other hand the investigated system can be a suitable model for studying the mechanical interaction of proteins and cell membranes during morphological transitions in cells.

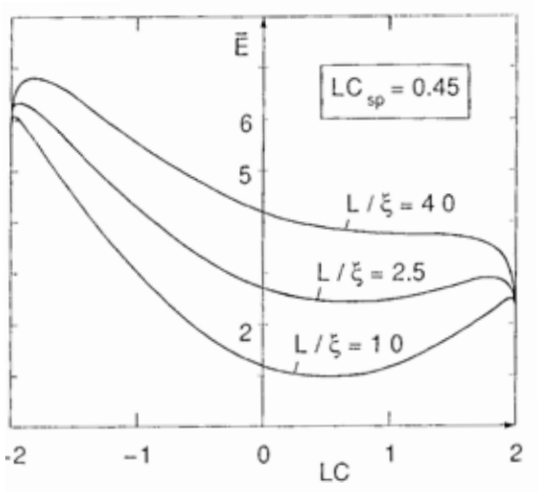

Fig. 4: *Domain induced budding in theory as described in [2]. With rising domain size L the local minimum in free energy for a curved domain becomes less pronounced. At a critical domain size* $L_{crit}=4\xi$ *the minimum disappears and the domain transforms into a spherical bud with a Radius* $R=1/C=0.5\ L_{crit}$. ξ *is an invagination length which depends on the properties of membrane and particles.*

References:

1. Holl, M. B. (2008). Cell Plasma Membranes and Phase Transitions. In G. Pollack & W.-C. Chin (Eds.), Phase Transitions in Cell Biology (pp. 171-181). Springer Netherlands.

2. Reinhard Lipowsky. (1992). Budding of membranes induced by intramembrane domains. J. Phys. II France, 2(10), 1825-1840.

3. Angelova, M. I., Soléau, S., Méléard, P., Faucon, F., & Bothorel, P. (1992). Preparation of giant vesicles by external AC electric fields. Kinetics and applications. In C. Helm, M. Lösche, & H. Möhwald (Eds.), Trends in Colloid and Interface Science VI (Vol. 89, pp. 127-131).

4. Westerhausen, C., Strobl, F. G., Herrmann, R., Bauer, A. T., Schneider, S. W., Reller, A., Wixforth, A., et al. (2012, March 7). Chemical and Mechanical Impact of Silica Nanoparticles on the Phase Transition Behavior of Phospholipid Membranes in Theory and Experiment. Biophysical journal. (Vol. 102, pp. 1032-1038).

Contact
Florian Strobl
Wixforth group
Universität Augsburg
Chair for Experimental Physics I
Universitätsstr. 1
86159 Augsburg
florian.strobl@physik.uni-augsburg.de

Bowling in Santa Barbara

Wine tasting in California

Excursion to Channel Islands National Park

Pacific coast line

Venice International University

Bavarian restaurant

Hiking weekend in the Dolomites

Stunning views

Networking beyond Science

An attractive social program, mostly self-organized by the PhD students, complemented the scientific part of the JNN 2012. Joint activities like sports, city tours or hiking strengthened the ties between the German and the Californian students. As a unique feature of the JNN, all participating students hosted a partner from abroad, i.e., the Californian participants provided accommodation for the German visitors and vice versa. This led to an intensive intercultural exchange, creating a strong personal network with benefits beyond science.

California...

The evenings and weekends in Santa Barbara gave the students a lot of opportunities to get together and travel around. Besides recreational activities such as barbecue or bowling, the German students explored some of the Californian attractions: They tasted the Californian wine at the famous wineries, hiked in the spectacularly beautiful Channel Islands National Park, enjoyed the stunning views along the coastline of Big Sur, and visited Monterey and Los Angeles – popular local tourist destinations.

Santa Barbara, University Campus

Bavaria...

The Californian students received a warm welcome in Munich with a typical Weisswurst breakfast. Joint activities like a late summer barbecue helped to connect JNN participants and CeNS students and supervisors. In addition, there were plenty of opportunities to experience Bavarian culture: A guided city tour in Munich gave the Californian participants a first glimpse of Bavarian history and traditions, including surprising similarities between Bavarians and Texans. Further highlights were the obligatory visit of the Oktoberfest, an excursion to Ludwig II's dream castle Neuschwanstein as well as an evening in a typical Bavarian restaurant after a guided tour at the Deutsches Museum.

Munich and the Alps

... and beyond

Blue sky, Mediterranean sun and wonderful views over the mountains - a weekend trip to the Dolomites offered perfect conditions for hiking tours at all levels. During the CeNS workshop in Venice, the German and Californian students enjoyed the magnificent scenery of the city and the special atmosphere when taking the vaporetto to the conference location. After intense days full of science, the evenings were devoted to getting lost in this fascinating system of narrow alleys and canals and to enjoying typical Italian food and life style.

Venice, Piazza San Marco

Students' Voices

"The peer training sessions were well organized and intellectually stimulating. Though I was unfamiliar with most of the subject matter, the instructors were able to clearly explain the details of their work and answer all of my questions. Some of the modules were directly applicable to my research and gave me new ideas and different ways of looking at things, which may help my research in the future."

"The technical facilities available at the LMU, TUM and elsewhere were very impressive... Housing accommodations were fantastic, and my host could not have been more hospitable... The recreational/social aspects of the program were fantastic. The weekend trip to Bozen was a great success and the Oktoberfest was one of the best experiences of my life. "

"Just the fact that different people with different scientific background were listening to my talk, was a great time to practice how to present my data and to learn answering questions."

"The recreational events during the program were particularly well organized. We could choose among several sightseeing programs. I would like to thank US PhD students for providing their cars for the long journeys."

"The JNN program was really great in terms of getting to know people and seeing how students in the US work. It also gave a nice overview of the quite diverse research in nanotechnology."

"The Venice Workshop provided interesting exposure to a diverse base of research. The breadth of the ties between CeNS and UCSB was surprising. For me, participation in the workshop solidified the heartening welcome to the CeNS research family that had been extended in the first week of the JNN program."

"I had an absolutely fantastic time in Munich and Venice during the program, and I am so grateful that I got to be a part of it. The scientific aspects of the program were stimulating and beneficial, and the recreational/cultural aspects left little to be desired. My thanks go out to all of the students, professors and coordinators who worked to make this program such an unforgettable experience."

"Overall an excellent program, and I feel very lucky to have had the opportunity to participate. It broadened my knowledge of nanoscience/research, and gave me the opportunity to make many new friends."

Contact

Scientific Organizers

CeNS

Prof. Tim Liedl
Physics Department LMU & CeNS
Ludwig-Maximilians-Universität (LMU) München
Geschwister-Scholl-Platz 1
D-80539 München, Germany
tim.liedl@physik.lmu.de
http://softmatter.physik.lmu.de/tiki-index.php?page=GroupLiedlHome

Prof. Alexander Holleitner
Physics Department TUM & CeNS
Technische Universität (TUM) München
Butenandtstr. 5-13, 81377 München
holleitner@wsi.tum.de
www.wsi.tum.de/Research/HolleitnergroupE24/tabid/166/Default.aspx

CNSI/UCSB

Prof. Deborah Fygenson
University of California, Santa Barbara
Physics Department
Santa Barbara, CA 93106
2419 Broida Hall
deborah@physics.ucsb.edu
http://web.physics.ucsb.edu/~deborah/index.html

Program Coordinators

CeNS / LMU

Dr. Susanne Hennig
Managing Director
Center for NanoScience (CeNS)
Ludwig-Maximilians-Universität (LMU)
Geschwister-Scholl-Platz 1
80539 Munich, Germany
hennig@cens.de
www.cens.de

CNSI/UCSB

Holly Woo
Assistant Director, Administration
California NanoSystems Institute (CNSI)
Elings Hall, Room 3245
University of California, Santa Barbara, CA 93106-6105
woo@cnsi.ucsb.edu
www.cnsi.ucsb.edu

The JNN 2012 was supported by


LMU
LUDWIG-
MAXIMILIANS-
UNIVERSITÄT
MÜNCHEN

UNIVERSITY OF CALIFORNIA
SANTA BARBARA